Development of High-Sensitive Immunoassay on Paper-Based Analytical Devices

Sumamal CHARERNCHAI

Graduate School of Advanced Science and Technology

Japan Advanced Institute of Science and Technology

Doctoral Dissertation

Development of High-Sensitive Immunoassay on Paper-Based Analytical Devices

Sumamal CHARERNCHAI

Supervisor: Professor Yuzuru Takamura

Graduate School of Advanced Science and Technology
Japan Advanced Institute of Science and Technology
Materials Science

September 2022

Abstract

Microfluidic paper-based analytical devices (μPADs) are promising biosensors that may be used in a variety of bioanalytical applications. Despite the benefits of being affordable, low-volume, and portable, there are restrictions, including issues with large-scale production, multi-step operation, and particularly detection sensitivity, that may pose difficulties for users.

To address those critical issues, a new μPAD for automating competitive enzyme-linked immunosorbent assay (ELISA) for small-sized target detection was developed. Simple, precise, and rapid device fabrication was achieved by laser-cutting technology. A Sucrose valve was utilized to automate the sequential delivery of reagents, providing simple user-operation. The device was demonstrated with Aflatoxin B_1 (AFB_1) antigen, which is a hydrophobic toxin and cancer-causing agent. During an examination of various parameters, a new sample-loading method, or the so-called Direct Dropping of Sample on Antibody Location (DDoAb), was discovered to allow minimization of sample volume to 0.6 μL, while eliminating the possible loss of a target molecule by adsorption on the membrane, thus improving detection sensitivity. Under the optimization conditions, the device achieved a limit of detection of 0.1 ng/mL or 60 fg, which is 2-4 orders of magnitude lower than other reports.

To further advance the sensitivity of μPAD to an ultimate level of single molecule detection, a new method for digital counting of molecules on μPAD was proposed. Streptavidin-conjugated alkaline phosphatase (SA-ALP) was used as an analyte model. Without the need for an expensive femtoliter-sized chambers, digital counting of SA-ALP was successfully conducted using enzymatic reaction, inexpensive materials, and general laboratory equipment. This simple and low-cost digital counting platform shows potential use in other bioanalytical applications and other target molecules.

Keywords: μPADs, Automated ELISA, Small-sized target, Aflatoxin B_1, Digital counting

Acknowledgements

First, I would like to express my sincerest respect and appreciation to my supervisor, *Professor Yuzuru Takamura* for his wisdom, generous guidance, suggestions, and continuous supports throughout my studies at JAIST. Along with his precise research supervision, I have always considered myself fortunate to have been in his laboratory as his kindness has inspired me to personal growth. Likewise, I would like to thank *Assistant Professor Hirose Daisuke*, *Mrs. Kiyomi Kosugi*, and all members of Takamura Lab for their generous assistance throughout my time at JAIST.

I would also like to thank *Professor Phan Trong Tue* and *Dr. Miyuki Chikae* for their assistance, advice, and valuable discussions, especially in the initial development of my research. Also, my appreciation goes to *Mr. Taniguchi Shunpei* for his assistance in the laser cutting instrumentation.

I am also grateful to *Professor Toshifumi Tsukahara, Professor Matsumura Kazuaki, Professor Eijiro Miyako,* and *Professor Masayasu Suzuki* from the University of Toyama, my thesis committee members, for giving valuable time and suggestions.

I sincerely appreciate the Doctoral Research Fellowship (DRF) and Mitani Scholarship Foundation for financially sponsoring me during these 3 years of my PhD study at JAIST.

I dedicate this to my family. I am truly thankful to my mother, *Sawitree*, and aunties *Suthida* and *Sujaree Thaneerat* for all the sacrifices they made to help me throughout my education. I am grateful for the unconditional love and support of my father, *Rattichai* and sister, *Sudarat Charoenchai*. I am especially affectionately thankful to *Mr. James Philip Rosenberg,* my fiancé who has been a heartfelt infinite support, tender love, and continuous care the entire time I have studied and lived in Japan. Because of all of them, every of my achievements are more meaningful.

Finally, I am thankful to everyone who has helped me not only with my studies but also with my life during my studies from Thailand to Japan. I appreciate friendship and thoughtfulness from everyone. With that, I am truly grateful from the bottom of my heart.

Autumn 2022

Sumamal Charernchai

Contents

Pages

Abstract i

Acknowledgements ii

CHAPTER I GENERAL INTRODUCTION 1

1.1 Introduction of paper-based analytical devices 1

1.1.1 Fabrication method 3

1.1.2 Sequential reagent delivery 6

1.1.3 Colorimetric detection 7

1.2 Introduction of immunoassay and its application 9

1.3 Analog and digital counting in biomolecule 11

1.4 Single molecule detection 12

1.4.1 Direct localization of molecules 14

1.5 Research objectives 16

1.6 Dissertation organization 18

1.7 References 20

CHAPTER II AUTOMATED COLORIMETRIC COMPETITIVE ELISA-µPADs WITH HIGH SENSITIVITY FOR SMALL-SIZE TARGET DETECTION 25

2.1 Introduction 25

2.2 Objective 27

2.3 Experimental 28

2.4 Results and discussions 38

2.4.1 Study of the device structure 41

2.4.2 Effect of sample-loading method 43

2.4.3 Optimization of reagents 47

2.4.4 Automated detection of AFB_1 51

2.4.5 Detection of spiked-AFB_1 soy sauce 53

2.5 Conclusion 55
2.6 References 56

CHAPTER III DIGITAL COUNTING ENZYNMATIC-μPAD 60
3.1 Introduction 60
3.2 Objective 62
3.3 Experimental 63
3.4 Results and discussions 68
3.4.1 The principle of digital counting on a μPAD for single-molecule detection 68
3.4.2 Optimization of the conditions for enzymatic reaction 69
3.4.3 Digital Counting on a μPAD for SA-ALP 73
3.5 Conclusion 75
3.6 References 76
CHAPTER IV GENERAL CONCLUSION 78
LIST OF PUBLICATIONS 79

CHAPTER I

GENERAL INTRODUCTION

This chapter presents an overview of paper-based analytical devices (μPADs), immunoassay and its applications, signal counting methods for biomolecule detection, and single molecule detection (SMD) approaches. Microfluidic paper-based analytical devices (μPADs) are popular due to several advantages, including their low cost, low volume, and portability. The fabrication methods, sequential reagent delivery, and analysis methods are mentioned. Additionally, the basis of immunoassay which is a common biological technique, ELISA, and its application are discussed. To advance the sensitivity of the device, general information about analog and digital counting in biomolecules is described, as well as approaches for single molecule detection. Finally, a discussion of the current issues with these techniques and the research objectives is presented.

1.1 Introduction of paper-based analytical devices (μPADs)

Over the centuries, paper has been used for a range of analytical applications, such as litmus paper as a pH indicator [1]. In 2007, patterned-paper was first reported as a platform for inexpensive, low-volume, and portable bioassays by Whitesides and colleagues [2]. This patterned-paper, or so-called microfluidic paper-based analytical device (μPAD), was created by separating defined areas of hydrophilic paper with hydrophobic lines, or "walls," that control the spatial flow

of biological fluids and enable fluid transport through capillary action, as shown in Figure 1.1. Since then, research on μPADs has continued to increase in popularity as a promising analytical tool for numerous applications.

Figure 1.1 Patterned paper, or so-called microfluidic paper-based analytical device (μPAD), after absorbing Waterman red ink (5 μL) by capillary action. Adapted with permission from ref. 2. Copyright © 2007 WILEY‐VCH Verlag GmbH & Co. KGaA, Weinheim.

Although μPADs have been used to overcome crucial analytical problems inside laboratory conditions, some limitations, e.g., large-scale production, on-site detection, and detection sensitivity, may pose obstacles to general users. As a result, the fabrication method, sequential reagent delivery, and analytical method are important issues for continued research to broaden the practical application of μPADs.

1.1.1 Fabrication methods

While the Whitesides group's work is widely acknowledged as establishing the µPAD field, the device was fabricated by utilizing photolithography to accurately create a hydrophobic barrier on chromatography paper. Although this fabrication method was useful for creating micropatterning devices, the requirements of many hours of complicated procedures and costly facilities (e.g., cleanrooms) hampered its potential use for mass production and device development in resource-limited settings.

More recently, several approaches for fabrication of µPADs have been reported. Generally, these methods involve either patterning a hydrophobic barrier on the paper substrate (e.g., wax-printing[3], inkjet-printing[4], stamping[5], screen-printing[6]) or shaping and cutting the paper to construct the fluidic channel (e.g., laser-cutting, laser-etching). Among these methods, wax-printing has been the most commonly used method [7], because of its low-cost patterning material and large-scale production capabilities. However, recent discontinuation of the solid wax printer by the manufacturer [8], together with no comparable affordable wax printers on the market, may present production challenges for wax-printed µPAD.

Alternatively, laser shaping is a technology that can rapidly and conveniently create high-resolution devices. The two major methodologies for laser device fabrication are laser cutting and laser etching. Laser cutting allows the production of a stand-alone µPAD, while laser etching involves the removal of a particular thickness of paper substrate. The hydrophobic barrier on the µPAD was

created using a laser technology by removing the nitrocellulose membrane (NCM) on a conventional NCM-plastic backing from the cutline of the designed pattern, as shown in Figure 1.1.1.1.

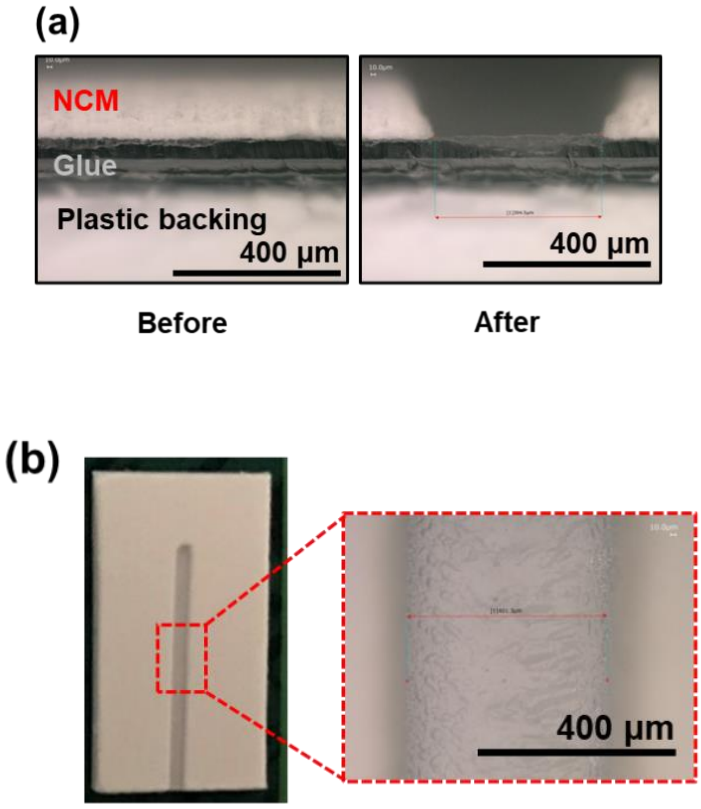

Figure 1.1.1.1 Images of laser-etching nitrocellulose membrane (NCM). (a) Cross section of conventional NCM before and after creating a barrier line. (b) Top view of barrier line.

While laser cutting demonstrates great promise in terms of ease of use, high reproducibility, and high accuracy, the residues in the fume from the laser cutting process could interfere with some detection assays.

As shown in Figure 1.1.1.2, a strong purple color appeared on the laser-cut membrane after dropping BCIP/NBT (5-bromo-4-chloro-3-indoxyle phosphate/nitro blue tetrazolium chloride). This was an indication that some substance in fumes from laser cutting catalyzes the reaction of the substrate (BCIP/NBT) and changes its color.

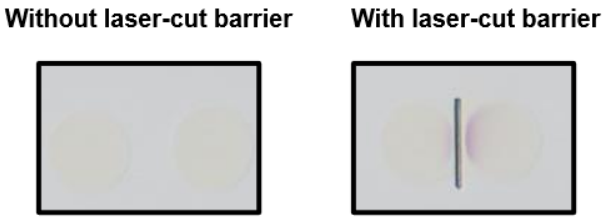

Figure 1.1.1.2 Color changing of enzymatic substrate (BCIP/NBT) on the without and with laser-cut barrier membranes.

The fume from the laser cutting procedure, on the other hand, can be simply washed away with buffer, as shown in Figure 1.1.1.3. Consequently, the combination of the laser technology combined with a commercially available NCM-plastic backing membrane enables the simple and rapid fabrication of µPADs.

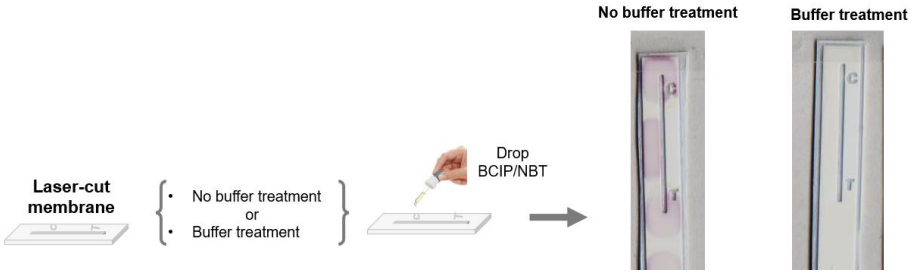

Figure 1.1.1.3 Color changing of enzymatic substrate on the no buffer treatment, and buffer treatment laser-cut membrane.

1.1.2 Sequential reagent delivery

While lowering the cost and volume of reagents, μPADs are intended to increase the simplicity for the use of traditional assays, enabling detections to be performed by general-users in limited-resource situations or on-site measurements. Especially for detections that involved multiple-steps assay, sequential delivery of reagents on μPADs is necessary for simplified device operation.

Geometry and chemical-based approaches are frequently used to control the sequential delivery of reagents on μPADs. In geometry-based approaches, flows of reagents are controlled by the physically modified paper itself. This includes alterations to the paper such as channel length, channel width, flow path, membrane orientation, and membrane porous density[9]. Reagent delivery in chemical-based approaches is determined by the chemical characteristics of the material. For example, Figure 1.1.2 shows the operation of dissolvable material in chemical-based approach.

Several chemicals, such as surfactants[10], polymers[11], and sugars[12], have been used to control reagent delivery time due to their solubilities. Among these chemicals, sugar exhibits the most outstanding choices because it is inexpensive, widely available, and frequently employed in immuno-devices as a bulking agent and preservative. As a result, sugar was used to chemically control the reagent delivery in our μPADs.

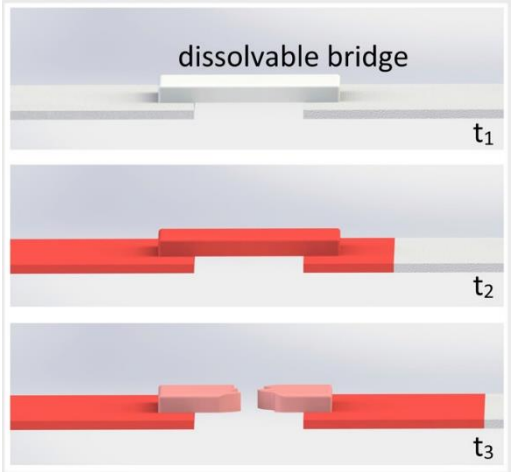

Figure 1.1.2. Operation of chemical-based approaches using the dissolubility of sugar. The dissolvable bridge (sugar) dissolves to a permanent shut-off state after passing a well-defined volume of fluid from the feeder material to the delivery material. Adapted with permission from ref. 12. Copyright © 2013, American Chemical Society

1.1.3 Colorimetric detection

Several detection methods, e.g., electrochemistry, luminescence, Raman spectroscopy, and colorimetric detection, have been incorporated into μPADs. Among these methods, colorimetry has been one of the most common detection methods used in clinical or diagnostic assays[13] due to its simplicity, ease of operation, and ability to meet the basic needs for on-site detection without complex equipment. Colorimetric detection typically implies visual observation of a reaction's change in color. With the naked eye or a visual aid, the color changes can be employed in qualitative or quantitative analysis.

Colorimetric interpretation of the test results can be measured by distance[14] or intensity-based signal[15], as shown in Figure 1.1.3. The distance-based μPADs determine sample concentration by measuring the length or distance of a colored (or loss of color) band that develops along the channel. The intensity-based μPADs determine the concentration of samples from the absolute amount of signal.

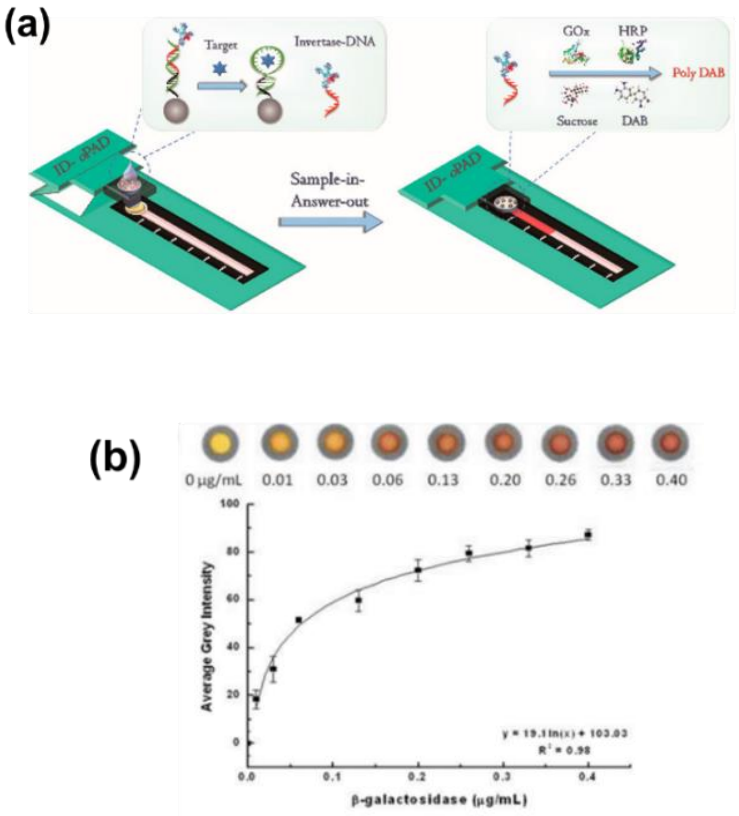

Figure 1.2.3 Colorimetric interpretation of the test results. (a) Distance-based signal. Adapted with permission from ref 14. Copyright © 2017, American Chemical Society. (b) Intensity-based signal of *β*-galactosidase enzyme. Adapted with permission from ref 15. Copyright © 2012, American Chemical Society

1.2 Introduction of immunoassay and its application

Immunoassays represent analytical methods that rely on antibody-antigen molecular interactions for the detection of target analytes[16]. Due to their high sensitivity and specificity for bioanalytical detection, immunoassays have been used in a range of applications including diagnostics, drugs and pharmaceuticals, environmental monitoring, and food safety.

One of the most well-known classifications for immunoassays is to use the configuration. Examples of the standard configurations of an immunoreaction are the sandwich, competitive, and indirect types[17], as shown in Figure 1.2.

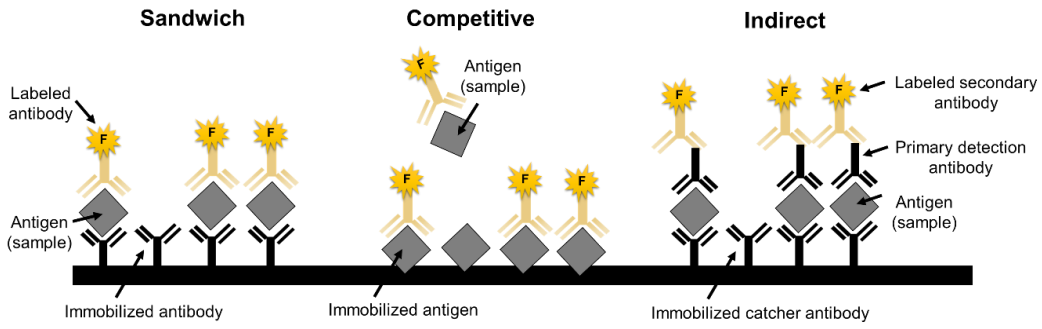

Figure 1.2 Sandwich, competitive and indirect configurations in immunoassay.

Each immunoreaction configuration has its own advantages, limitations, and suitability. For instance, the sandwich configuration provides high specificity since it utilizes two antibodies that recognize different epitopes on the same antigen, making it suitable for complex samples. The requirements for two antibodies to work successfully together, however, can be challenging at times. Moreover, the antigen target must be large enough to allow simultaneous binding of two

antibodies. Competitive configuration, on the other hand, is suitable for small-sized antigens. While competitive assays are simple since only one antibody is required, the labeling step may possibly result in inactivation of the antibody[18]. Indirect configuration offers high sensitivity because the use of secondary antibodies enabling signal amplification. This assay protocol, however, might be complicated because additional incubation steps with the secondary antibody are frequently necessary. Additionally, the use of secondary antibodies may result in cross-reactivity.

Molecules such as radioisotopes, enzymes, chemiluminescence, fluorescence, bioluminescence, and metal nanoparticles are commonly used to label antigens or antibodies in immunoassays. Among them, the enzyme labeling technique, also known as enzyme-linked immunosorbent assay (ELISA), is one of the most widely used and is considered the gold standard of immunoassays [19, 20]. Due to its high sensitivity, specificity, precision, and throughput, ELISA has been widely used for immunosensors for numerous analytes.

Many studies integrated ELISA with colorimetric detection and sequential delivery of reagents on µPADs, allowing for high specificity while being inexpensive, simple, and easy to use. Even so, the sensitivity of ELISA on µPAD remains a challenge, especially with an automated-ELISA µPAD at femtogram level sensitivity.

1.3 Analog and digital counting in biomolecule

Signal detection, as distinct from functional assay sensitivity, refers to the amplitude of the observable signal, without interpretation thereof[21]. Improving signal detection could lead to an improvement in the sensitivity of analyte measurement.

In conventional ELISA, signal readout typically necessitates a large number of target particles and/or enzyme labels to generate a detectable signal above background. This signal is proportional to the concentration of the bulk sample, and its value can be determined using a reference curve[22]. This signal detection approach is commonly referred to as “analog counting”, as shown in Figure 1.3(a). The sensitivity of analog counting in ELISA is generally limited to detecting picomolar (pM) concentrations of proteins [23].

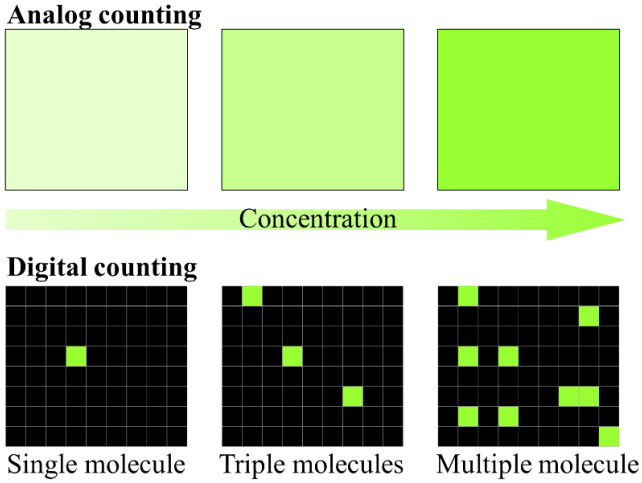

Figure 1.3 Signal detection. (a) Analog measurements give increasing intensity as the concentration increases. (b) digital measurements are independent of intensity and simply rely on a signal/no signal readout.

Digital counting is a method that literally counts the number of molecules[24], as shown in Figure 1.3(b). Each molecule confined within a femto-liter droplet chamber array generates a signal that can be counted. This signal is a direct representation of the presence or absence of each target molecule. This concept is also known as single molecule detection (SMD).

Although digital counting in ELISA (digital ELISA) has a 1000 times greater sensitivity than conventional ELISA[25], its application to an affordable sensing platform such as μPADs remains challenging due to the high cost and complexity isolating individual molecules and their signals for digital counting [26].

1.4 Single molecule detection

Single molecule detection (SMD) is indeed the ultimate goal in the quest to improve signal detection and the sensitivity of measurement. The current gold standard tool for ultrasensitive protein detection is digital ELISA using Single Molecule Arrays (Simoa)[27, 28], as shown in Figure 1.4.

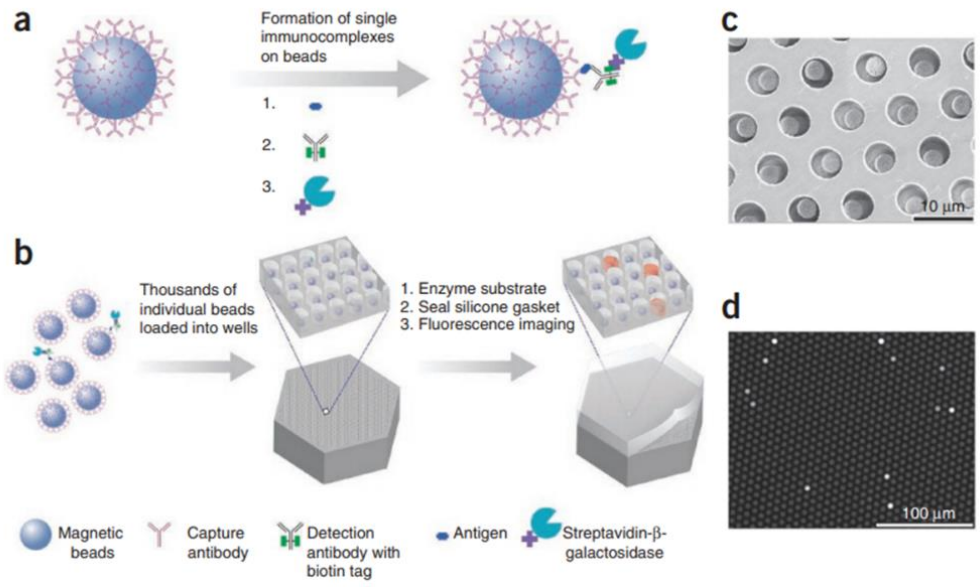

Figure 1.4 Digital ELISA based on arrays of femtoliter-sized wells. (a,b) Single protein molecules are captured and labeled on beads using standard ELISA reagents. (c) Scanning electron micrograph of a small section of a femtoliter-volume well array after bead loading. (d) Fluorescence image of a small section of the femtoliter-volume well array after signals from single enzymes are generated. Adapted with permission from ref 28. Copyright © 2010, Nature Publishing Group.

In digital ELISA, single proteins were detected using fluorescence imaging by capturing them on microscopic beads and labeling them with an enzyme, then isolating them in arrays of 50-femtoliter reaction chambers. The combination of signal amplification by enzyme and molecule confinement was essential in this strategy for achieving sub-femtomolar protein detection sensitivity. While digital ELISA in microarrays has been implemented in numerous clinical applications, this detection platform is currently not amenable for point-of-care technologies.

1.4.1 Direct localization of molecules

Recently, a simplified digital ELISA was reported on single molecule detection without the use of microarray for molecule localization [29]. The system referred to as catalyzed reporter deposition digital ELISA (CARD-dELISA), as shown in Figure 1.4.1.

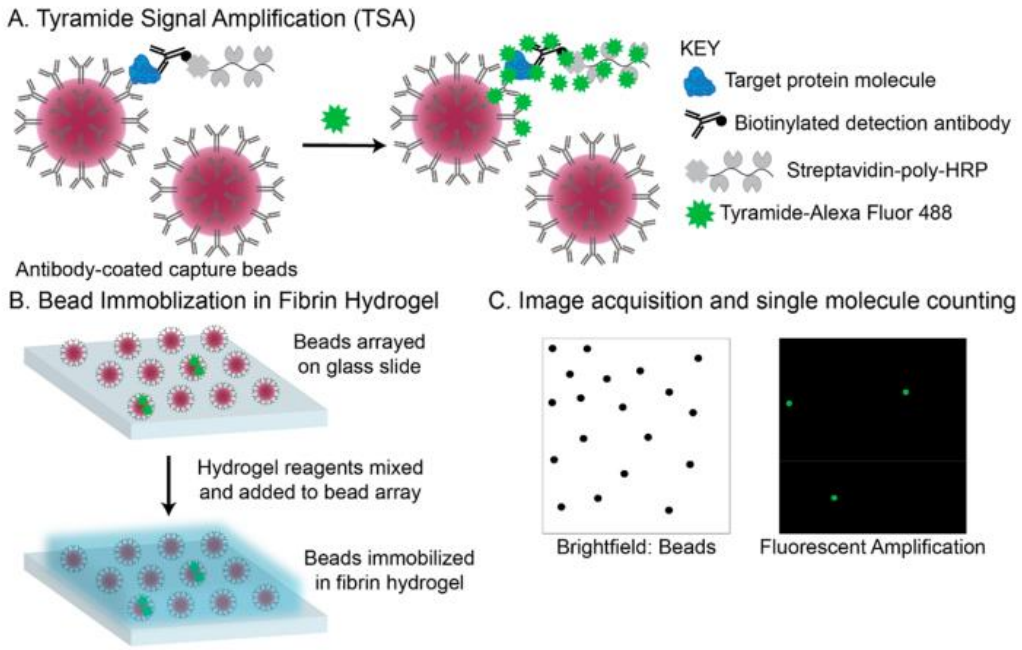

Figure 1.4.1 CARD-dELISA. (a) Tyramide signal amplification (TSA). (b) Bead immobilization in Fibrin Hydrogel. (c) Single molecule counting on fluoresce image. Adapted with permission from ref 29. Copyright © 2020, American Chemical Society.

In this system, on-bead signal generation using the CARD tyramide signal amplification (TSA) technique was integrated with bead immobilization in fibrin

hydrogels and single molecule counting on fluoresce image. While requiring multi-step processing procedures, the CARD-dELISA was successful in achieving ultrasensitive protein detection with a femtomolar dynamic range.

Bride amplification exhibits a promising direct localization of both target molecules and their amplified signals. Bride amplification can produce randomly distributed, clonally amplified clusters from fragments or mate-pair templates [30], as shown in Figure 1.4.2. In this method, two basic steps consist of (i) initial priming and extending of the single-stranded, single-molecule template, and (ii) the extension product from one primer forms a bridge to the other primer. Despite the fact that bridge amplification is commonly used to determine the series of base pairs in DNA (deoxyribonucleic acid), its work concept presents an opportunity for single molecule detection on membrane platforms, μPADs as an example.

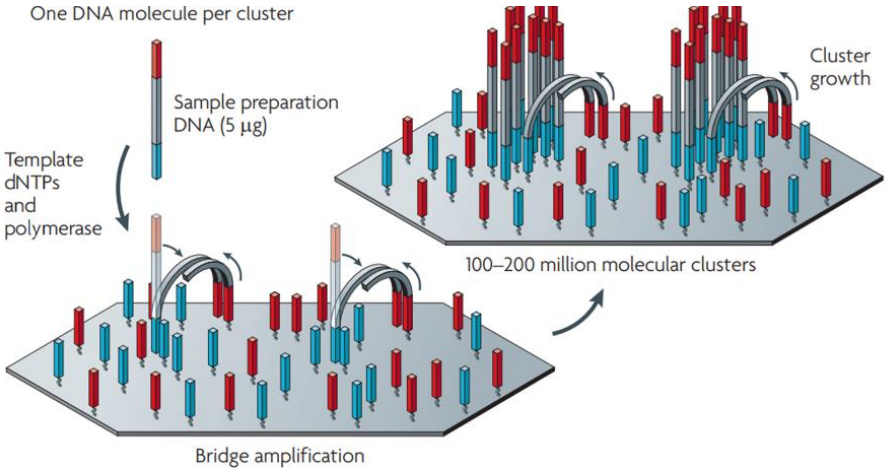

Figure 1.4.2 Bridge amplification. Adapted with permission from ref 30. Copyright © 2009, Nature Publishing Group.

While direct localization of signals such as CARD-dELISA and bridge amplification have shown their capability for single molecule detection, these technologies have yet to be incorporated into a simple, low-cost, and easy-to-use platform. μPADs, on the other hand, have those capabilities, but their sensitivity remains an issue. Therefore, more research towards signal amplification, direct localization of molecules, and digital counting on μPADs is crucial for addressing their sensitivity and single-molecule detection challenge.

1.5 Research objectives

The details of currents of automated colorimetric ELISA-μPADs, single molecule detection, and research objectives are presented below:

- **Current problem for automated colorimetric ELISA-μPADs**

Automated colorimetric ELISA-μPADs have attracted significant interest as a low-cost, simple-to-use, fast, and portable detection tool. The majority of automated colorimetric ELISA-μPADs reported detecting biomolecules in a sandwich format. The sandwich format has a number of advantages in its own right, including high specificity due to the use of two antibodies and flexibility for complex sample analysis. This format, on the other hand, can also pose a challenge to detecting small target molecules, whose small molecular structure prevents two antibodies from binding simultaneously. Competitive ELISA is a more preferable detection format for small molecule detection. However, only a few studies have demonstrated competitive ELISA in an automated colorimetric detection on

μPADs, especially for small-size target detection. In fact, high sensitivity detection of many small-size target molecules is critical for clinical diagnostics, environmental monitoring, food safety, and other applications. Therefore, herein, an automated colorimetric competitive ELISA-μPADs has been developed for small-size target detection.

- **Current problem for single molecule detection**

Digital ELISA has proven to be a promising method for achieving ultra-sensitive single-molecule detection. While digital ELISA is a highly sensitive technology, it is also a sophisticated and expensive platform for general users or setups with limited resources. More recently, the relatively simpler and lower-cost single molecule detection method, namely CARD-dELISA, was reported. The utilization of magnetic beads and the multi-step processes of CARD-dELISA are still challenging in practical applications. Bridge amplification has shown its capability for direct molecule localization and single molecule detection, however, this technology has yet to be applied into an affordable platform. As a result, there is a need to develop a simple, inexpensive, easy-to-use single molecule detection device.

- **Objectives**

  To solve these issues, the objectives of this research are:

  - To develop an automated colorimetric competitive ELISA-µPADs with high sensitivity for small-size target detection
  - To develop a new method for digital counting of single molecules on µPAD

1.6 Dissertation organization

Chapter I presents a general introduction to µPADs, including immunoassay and its applications, analog and digital counting methods for biomolecule detection, and signal amplification for single molecule detection (SMD). In this part, the development of key research in µPADs, sequential delivery of reagents, and single molecule detection approaches is summarized. Finally, current issues with this method and the research goal are discussed.

Chapter II presents the development of an automated colorimetric competitive ELISA-µPADs with high sensitivity for small-size target detection. Aflatoxin B_1 (AFB_1), a small-size antigen, was used as a target in this chapter. The importance of AFB_1 detection is also described. The results of optimization, the effect of sample loading methods, and real sample matrix detection are presented in the analog measurement.

Chapter III introduces the study of digital counting on µPADs. This chapter shows development of direct localization of target molecules and their signals on µPADs before digital counting the signal by microscope. The preliminary results from digital counting streptavidin-conjugated alkaline phosphatase (SA-ALP) molecules on µPADs is presented.

Chapter IV gives some general conclusions and notable points throughout the dissertation.

1.7 References

[1] A. Abdollahi-Aghdam, M.R. Majidi, Y. Omidi, Microfluidic paper-based analytical devices (μPADs) for fast and ultrasensitive sensing of biomarkers and monitoring of diseases, Bioimpacts, 8 (2018) 237-240.

[2] A.W. Martinez, S.T. Phillips, M.J. Butte, G.M. Whitesides, Patterned Paper as a Platform for Inexpensive, Low-Volume, Portable Bioassays, Angewandte Chemie International Edition, 46 (2007) 1318-1320.

[3] E. Carrilho, A.W. Martinez, G.M. Whitesides, Understanding Wax Printing: A Simple Micropatterning Process for Paper-Based Microfluidics, Analytical Chemistry, 81 (2009) 7091-7095.

[4] A. Apilux, Y. Ukita, M. Chikae, O. Chailapakul, Y. Takamura, Development of automated paper-based devices for sequential multistep sandwich enzyme-linked immunosorbent assays using inkjet printing, Lab on a Chip, 13 (2013) 126-135.

[5] V.F. Curto, N. Lopez-Ruiz, L.F. Capitan-Vallvey, A.J. Palma, F. Benito-Lopez, D. Diamond, Fast prototyping of paper-based microfluidic devices by contact stamping using indelible ink, RSC Advances, 3 (2013) 18811-18816.

[6] Y. Sameenoi, P.N. Nongkai, S. Nouanthavong, C.S. Henry, D. Nacapricha, One-step polymer screen-printing for microfluidic paper-based analytical device (μPAD) fabrication, Analyst, 139 (2014) 6580-6588.

[7] E. Noviana, T. Ozer, C.S. Carrell, J.S. Link, C. McMahon, I. Jang, C.S. Henry, Microfluidic Paper-Based Analytical Devices: From Design to Applications, Chemical Reviews, 121 (2021) 11835-11885.

[8] J.S. Ng, M. Hashimoto, Fabrication of paper microfluidic devices using a toner laser printer, RSC Advances, 10 (2020) 29797-29807.

[9] P. Mehrdel, H. Khosravi, S. Karimi, J.A. Martínez, J. Casals-Terré, Flow Control in Porous Media: From Numerical Analysis to Quantitative μPAD for Ionic Strength Measurements, Sensors, 21 (2021).

[10] H. Chen, J. Cogswell, C. Anagnostopoulos, M. Faghri, A fluidic diode, valves, and a sequential-loading circuit fabricated on layered paper, Lab on a Chip, 12 (2012) 2909-2913.

[11] S. Jahanshahi-Anbuhi, A. Henry, V. Leung, C. Sicard, K. Pennings, R. Pelton, J.D. Brennan, C.D.M. Filipe, Paper-based microfluidics with an erodible polymeric bridge giving controlled release and timed flow shutoff, Lab on a Chip, 14 (2014) 229-236.

[12] J. Houghtaling, T. Liang, G. Thiessen, E. Fu, Dissolvable bridges for manipulating fluid volumes in paper networks, Analytical chemistry, 85 (2013) 11201-11204.

[13] E. Evans, E.F.M. Gabriel, W.K.T. Coltro, C.D. Garcia, Rational selection of substrates to improve color intensity and uniformity on microfluidic paper-based analytical devices, Analyst, 139 (2014) 2127-2132.

[14] T. Tian, Y. An, Y. Wu, Y. Song, Z. Zhu, C. Yang, Integrated Distance-Based Origami Paper Analytical Device for One-Step Visualized Analysis, ACS Applied Materials & Interfaces, 9 (2017) 30480-30487.

[15] J.C. Jokerst, J.A. Adkins, B. Bisha, M.M. Mentele, L.D. Goodridge, C.S. Henry, Development of a Paper-Based Analytical Device for Colorimetric

Detection of Select Foodborne Pathogens, Analytical Chemistry, 84 (2012) 2900-2907.

[16] A. Kapoor, S. Prabhakar, Chapter 7 - Immunoassays applications, in: Inamuddin, R. Boddula, A.M. Asiri (Eds.) Green Sustainable Process for Chemical and Environmental Engineering and Science, Elsevier, 2021, pp. 161-173.

[17] H.J. Cruz, C.C. Rosa, A.G. Oliva, Immunosensors for diagnostic applications, Parasitology Research, 88 (2002) S4-S7.

[18] S. Sakamoto, W. Putalun, S. Vimolmangkang, W. Phoolcharoen, Y. Shoyama, H. Tanaka, S. Morimoto, Enzyme-linked immunosorbent assay for the quantitative/qualitative analysis of plant secondary metabolites, J Nat Med, 72 (2018) 32-42.

[19] T. Lakshmipriya, S.C.B. Gopinath, T.-H. Tang, Biotin-Streptavidin Competition Mediates Sensitive Detection of Biomolecules in Enzyme Linked Immunosorbent Assay, PLOS ONE, 11 (2016) e0151153.

[20] S.K. Vashist, J.H.T. Luong, Chapter 1 - Immunoassays: An Overview, in: S.K. Vashist, J.H.T. Luong (Eds.) Handbook of Immunoassay Technologies, Academic Press, 2018, pp. 1-18.

[21] Q. Ruan, J. Macdonald Patrick, M. Swift Kerry, Y. Tetin Sergey, Direct single-molecule imaging for diagnostic and blood screening assays, Proceedings of the National Academy of Sciences, 118 (2021) e2025033118.

[22] R. Nouri, Z. Tang, W. Guan, Calibration-Free Nanopore Digital Counting of Single Molecules, Analytical Chemistry, 91 (2019) 11178-11184.

[23] D.M. Rissin, D.R. Fournier, T. Piech, C.W. Kan, T.G. Campbell, L. Song, L. Chang, A.J. Rivnak, P.P. Patel, G.K. Provuncher, E.P. Ferrell, S.C. Howes, B.A. Pink, K.A. Minnehan, D.H. Wilson, D.C. Duffy, Simultaneous detection of single molecules and singulated ensembles of molecules enables immunoassays with broad dynamic range, Analytical chemistry, 83 (2011) 2279-2285.

[24] L. Chang, D.M. Rissin, D.R. Fournier, T. Piech, P.P. Patel, D.H. Wilson, D.C. Duffy, Single molecule enzyme-linked immunosorbent assays: theoretical considerations, J Immunol Methods, 378 (2012) 102-115.

[25] G.C. O'Connell, M.L. Alder, C.G. Smothers, C.H. Still, A.R. Webel, S.M. Moore, Use of high-sensitivity digital ELISA improves the diagnostic performance of circulating brain-specific proteins for detection of traumatic brain injury during triage, Neurological research, 42 (2020) 346-353.

[26] J.M. Emory, Z. Peng, B. Young, M.L. Hupert, A. Rousselet, D. Patterson, B. Ellison, S.A. Soper, Design and development of a field-deployable single-molecule detector (SMD) for the analysis of molecular markers, The Analyst, 137 (2012) 87-97.

[27] L. Cohen, N. Cui, Y. Cai, P.M. Garden, X. Li, D.A. Weitz, D.R. Walt, Single Molecule Protein Detection with Attomolar Sensitivity Using Droplet Digital Enzyme-Linked Immunosorbent Assay, ACS Nano, 14 (2020) 9491-9501.

[28] D.M. Rissin, C.W. Kan, T.G. Campbell, S.C. Howes, D.R. Fournier, L. Song, T. Piech, P.P. Patel, L. Chang, A.J. Rivnak, E.P. Ferrell, J.D. Randall, G.K. Provuncher, D.R. Walt, D.C. Duffy, Single-molecule enzyme-linked

immunosorbent assay detects serum proteins at subfemtomolar concentrations, Nature Biotechnology, 28 (2010) 595-599.

[29] A.M. Maley, P.M. Garden, D.R. Walt, Simplified Digital Enzyme-Linked Immunosorbent Assay Using Tyramide Signal Amplification and Fibrin Hydrogels, ACS Sensors, 5 (2020) 3037-3042.

[30] M.L. Metzker, Sequencing technologies — the next generation, Nature Reviews Genetics, 11 (2010) 31-46.

CHAPTER II

AUTOMATED COLORIMETRIC COMPETITIVE ELISA-µPADs WITH HIGH SENSITIVITY FOR SMALL-SIZE TARGET DETECTION

This chapter reports a µPAD for automating the competitive enzyme-linked immunosorbent assay (ELISA) of small-sized target detection. This µPAD used a sucrose valve to automate the sequential delivery of reagents. To obtain high sensitivity, various sample loading positions were investigated, as well as reagent optimization. Dropping samples in zones of the device that had been prepared with an antibody-conjugated enzyme (ALP-Ab) before immersion in a running buffer, was found to improve detection sensitivity significantly. While improving the sensitivity, this new sample loading method reduces the sample volume to 0.6 µL.

Under the optimal conditions, the proposed device successfully automates competitive ELISA for the detection of aflatoxin B_1 (AFB_1) with a detection limit of 60 femtograms or 0.1 ng/mL. Furthermore, real sample measurement was also done in spiked-AFB_1 soy sauce.

2.1 Introduction

The first automated sandwich ELISA inkjet-printed µPAD was reported in 2013[1]. This device required only a single sample application, directly immersing

the device into a sample solution, to run the entire assay, as shown in Figure 2.1. The intensity of the insoluble color product from an alkaline phosphatase (ALP) reaction was used to determine the level of human chorionic gonadotropin (hCG) on the µPAD. The device achieved fully automated-sandwich ELISA with a limit of detection (LOD) of 1 ng/mL, using 70 µL of sample solution.

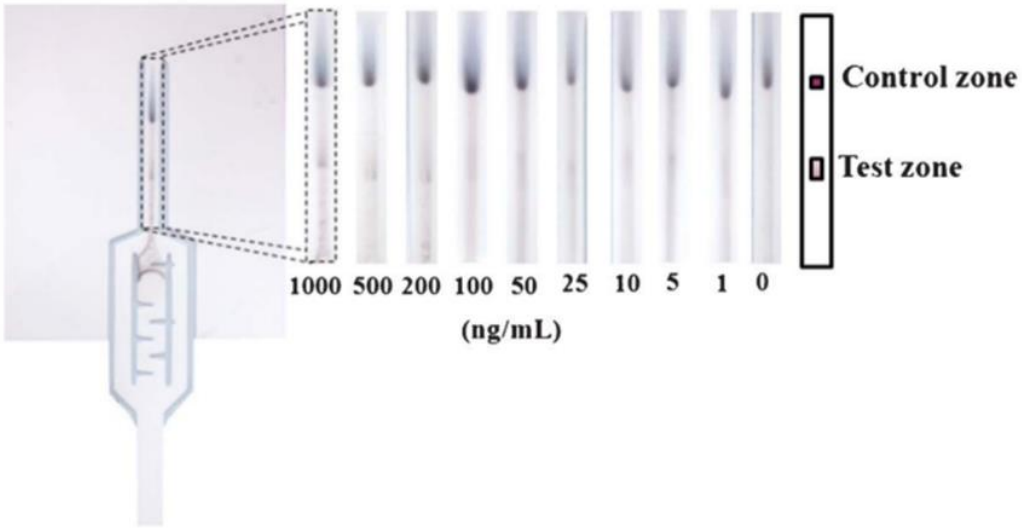

Figure 2.1 Automated sandwich ELISA-µPAD using intensity of the insoluble color product from an alkaline phosphatase (ALP) reaction. Adapted with permission from ref. 1. Copyright © 2013 Royal Society of Chemistry.

Since then, numerous colorimetric automated sandwich ELISA µPADs have been used in a variety of applications [2-5]. On the other hand, there have been a limited number of studies reported for automated-competitive ELISA µPADs for small-size target detection [6, 7], particularly in food toxins[8].

Aflatoxin B_1 (AFB_1) is a small hydrophobic molecule with a molecular weight of 312.3 Da[9]. Due to its carcinogenicity and immunosuppression capacity on humans and animals[10], AFB_1 is classified as a group 1 carcinogen by the International Agency for Research on Cancer (IARC) classification of carcinogenic substances[11]. AFB_1 contamination in foods (such as almonds, rice, cereals, and corn) has been a persistent problem worldwide[12]. As a result, monitoring AFB_1 levels is critical for public health.

In this work, an automated enzyme-enhanced competitive ELISA μPAD was developed for aflatoxin B_1 detection. The sucrose solution was utilized for automating the sequential delivery of reagents on the μPAD [13]. The proposed device was used in detection of AFB_1 in both of buffer and a Japanese soy-sauce matrixes under the optimal conditions.

2.2 Objective

The objective of this study is to develop an automated competitive ELISA-μPAD with high sensitivity for small-size target detection. AFB_1 was used as an antigen target. To improve the sensitivity of the detection, a study on the effects of sample-loading methods, and reagent optimizations is presented. To demonstrate the performance of the device, a real sample measurement in spiked-AFB_1 soy sauce was done.

2.3 Experimental

This section provides a detailed explanation of the chemicals, materials, and equipment used in this work, as well as information on reagent preparation, μPAD fabrication, and the detection method.

2.3.1 Chemicals, materials, and equipment

Analytical-grade reagents and 18 MΩ-cm resistance water (obtained from a Barnstrad Milli-Q purification system) were used throughout the experiments. Other chemicals are listed in Table 2.1.

Table 2.1 List of chemicals.

Chemicals	Suppliers
The BCIP/NBT (5- bromo-4-chloro-39-indolyphosphate p-toluidine salt, nitro-blue tetrazolium chloride) substrate solution	Nacalai Tesque (Kyoto, Japan)
Substrate buffer solution	Nacalai Tesque (Kyoto, Japan)
Methanol	Nacalai Tesque (Kyoto, Japan)
Alkaline phosphatase-labeling kit	Dojindo (Rockford, IL, USA)
Aflatoxin B_1−BSA conjugate from *Aspergillus flavus* (AFB_1-BSA)	Sigma-Aldrich (St. Louis, MO, USA)
Bovine serum albumin (BSA)	Sigma-Aldrich (St. Louis, MO, USA)
Anti-aflatoxin B_1 antibody	Abcam (Cambridge, UK)

Chemicals	Suppliers
Goat anti-mouse IgG H&L	Abcam (Cambridge, UK)
Boric acid	Wako (Japan)
Casein	Wako (Japan)
Sucrose	Wako (Japan)
Polyoxyethylene (20) sorbitan monolaurate (Tween 20)	Wako (Japan)
Tris(hydroxymethyl)aminomethane	Wako (Japan)
Sodium hydroxide	Wako (Japan)
Japanese soy sauce	Kikkoman (Japan)

The list of materials, equipment and suppliers that were used throughout the experiments is shown in Table 2.2.

Table 2.2 List of materials and equipment.

Equipment	Suppliers
Nitrocellulose membrane, immunopore RP, capillary flow 90-150 sec/4 cm, code number 78356403	GE Healthcare (Japan)
Absorbent pad, code number CFSP203000	EMD Millipore Corporation
Laser machine, VLS 3.50	Universal Laser Systems (Scottsdale, AZ, USA)
Laptop Computer, ThinkPad X240	Lenovo (Japan)

Equipment	Suppliers
Digital camera, G9X	Canon Inc. (Japan)
Desktop scanner, LiDE 220	Canon Inc. (Japan)
CorelDRAW software	Corel Corporation
ImageJ software	National Institutes of Health (Bethesda, MD, USA)
Digital hotplate/stirrer PMC 720	Barnstead Thermolyne Corporation
Oven, DKN301	Yamato (Japan)
pH meter, F-72 LAQUA	Horiba Scientific

2.3.2 Reagents preparation

The blocking solution was 1% (w/v) casein in milk in 50 mM boric acid buffer. Briefly, 5 mL 10 M NaOH was added to 800 mL milli-Q water. Next, 10 g of casein was added to the solution and heated at 60 °C with stirring at 800 rpm for 2 hours. After that, cool it down before adding 6.183 g of boric acid. The pH was adjusted to 8.5 and the solution final volume was adjusted to 1,000 mL. The blocking solution was stored for further use at 4°C.

The washing solution was 20 mM Tris-HCl buffer (pH 7.6) with 0.1 % (v/v) Tween. Briefly, 2.42 g of Tris was dissolved in 900 mL milli-Q water. After that, the solution was adjusted to pH 7.6 using 5 M HCl. The solution volume was

adjusted to 1,000 mL with milli-Q water. Finally, 1 mL of Tween 20 was added to the solution and mixed well. The washing solution was stored for further use at 4°C.

Alkaline phosphatase conjugated anti-aflatoxin B_1 antibody (ALP-Ab) was conjugated using an alkaline phosphatase-labeling kit purchased from Dojindo (Rockford, IL, USA) according to the manufacturer's instructions[14], and prepared at 15 μg/mL with 50 mM Tris-HCl buffer (pH 7.6) containing 1 % (v/v) BSA.

The test zone (TZ) was prepared by diluting AFB_1-BSA (stock solution at 5 mg/mL) with Tris-HCl buffer pH 7.6 to the desired concentration before use.

The control zone was 0.125 mg/mL of goat anti-mouse IgG. The commercial goat anti-mouse IgG at 2 mg/mL was diluted with 50 mM Tris-HCl buffer pH 7.6 before use.

The sucrose valve was 80% (w/v) of sucrose solution. 80 mg of sucrose was dissolved in 100 μL of milli-Q water.

The BCIP/NBT substrate was prepared by diluting the commercial BCIP/NBT with the substrate buffer (which is a Tris-HCl buffer solution containing Magnesium Chloride) at a ratio of 1:4 before use.

Running buffer was prepared with the substrate buffer containing 20 % (v/v) methanol and 0.1 % (v/v) BSA.

Standard AFB_1 sample was prepared by diluting the stock AFB_1 (1 mg/mL stored in acetonitrile) to the desired concentration with the running buffer.

Spiked AFB_1 soy sauce sample was prepared by diluting the stock AFB_1 (1 mg/mL stored in acetonitrile) to the desired concentration with the soy sauce.

2.3.3 µPADs fabrication

µPADs consisted of a reaction pad and an absorbent pad. The reaction pad was constructed by NCM with a 5 mm width and a 2.5 cm length. The pattern on the reaction pad was engraved by a laser. After patterning the reaction pad, the membrane was cleaned by soaking it in water for 30 min before drying it at 37 °C for 30 min.

To immobilize the test zone (TZ) and the control zone (CZ) on the devices, AFB_1-BSA and goat anti-mouse IgG (0.125 mg/mL at 0.3 µL) were manually spotted at the detection channel on the membrane at the TZ and CZ and allowed to dry for 30 min at room temperature (RT). Next, the membrane was soaked in the blocking and washing solution for 30 min at RT before drying at RT overnight.

To attach the absorbent pad to the reaction pad, a regular office stapler was used. For the application of sucrose valves, 0.6 µL of 80 % w/v sucrose solution was dropped onto the membrane for each valve. The sucrose valves were then allowed to dry at RT for 30 min. The basic structure of µPAD, consisting of TZ, CZ, and sucrose valve, is shown in Figure 2.3.3. The device was ready for further application of ALP-Ab, BCIP/NBT substrate, AFB_1 sample, and running buffer in the immunoassay.

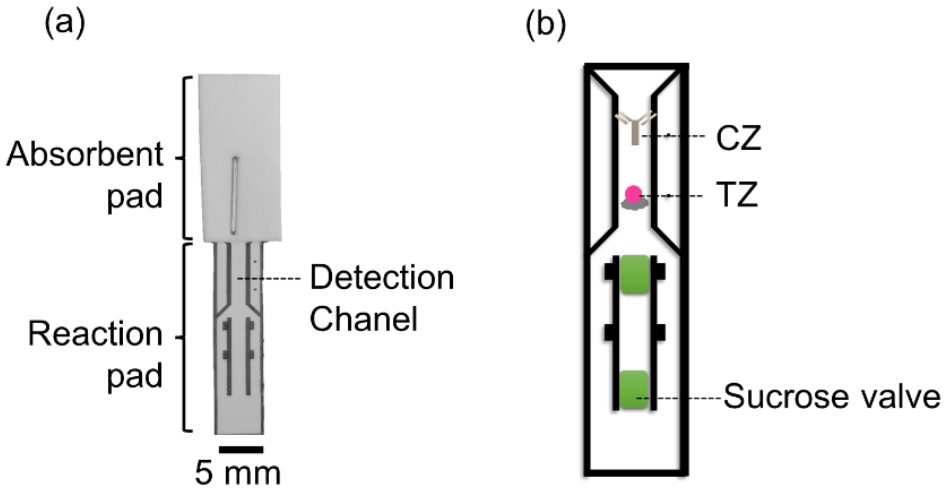

Figure 2.3.3 Basic structure of the μPAD. (a) A photograph of μPAD. (b) A reaction pad consisting of TZ, CZ, and sucrose valves.

2.3.4 Sample-loading method

All the devices in this section were prepared with the test zone (TZ, 0.5 mg/mL of AFB_1-BSA at 0.3 μL), the control zone (CZ, 0.125 mg/mL goat anti-mouse IgG at 0.3 μL), and sucrose valves (80 % w/v sucrose solution at 0.6 μL each valve).

For the experiment on the investigation of the effects of sample-loading methods, 10 μg/mL of ALP-Ab at 0.3 μL was dropped onto the membrane, as shown in Figure 2.3.4. This area on the membrane is the so-called ALP-Ab zone.

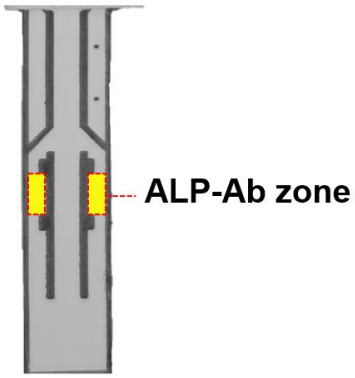

Figure 2.3.4 The ALP-Ab zone of the μPAD.

Sample solutions were applied in three distinct locations, as shown in Table 2.3. In the case (i), the device was immersed into a well plate of the sample solution directly. In cases (ii) and (iii), the sample solution was applied to the membrane first, then the device was dipped into a well plate containing running buffer (70 μL). After complete loading solutions from a well plate (70 μL of sample or running buffer), the BCIP/NBT substrate (1.5 μL) was manually applied to cover the detection channel on the device for colorimetric visualization.

Table 2.3 Sample-loading location and volume.

Case	Sample location	Total sample volume (μL)
(i)	in a well plate	70
(ii)	on the membrane at a location 1 mm below the ALP-Ab zones	0.6
(iii)	on the membrane at the ALP-Ab zones	0.6

For the experiment of direct mixing of the sample solution and ALP-Ab in a well plate, a mixture solution containing ALP-Ab (10 μg/mL at 0.6 μL) and sample solution (70 μL) was used. The device was dipped into this mixture. After finished loading the mixture from a well plate, the BCIP/NBT substrate (1.5 μL) was manually applied onto the detection channel.

For the experiment on confirmation of the position accuracy required for sample dropping, the devices were prepared with 10 μg/mL of ALP-Ab at 0.6 μL. The sample solution containing AFB_1 (0.3 μL each) was applied to various positions on the membrane. Next, the device was dipped in a well plate of running buffer (70 μL). Following the completion of the running buffer loading, the BCIP/NBT substrate (1.5 μL) was manually applied to the detection channel.

2.3.5 Optimization of reagents

For the test zone (TZ) condition, the volume (μL) and concentration of AFB_1-BSA were examined. All devices were prepared by the ALP-Ab at 15 μg/mL (0.3 μL each at the ALP-Ab zone). The samples (blank and 10 ng/mL AFB_1) at 0.3 μL each were applied to the ALP-Ab zones. To optimize the volume of TZ, AFB_1-BSA (1.5 mg/mL) was immobilized to the membrane at three different volumes (0.3, 0.6, and 1.2 μL). After applying ALP-Ab, samples, and loading 70 μL of running buffer, the BCIP/NBT substrate (1.5 μL) was manually applied to cover the detection channel on the device. To optimize the concentration of TZ, AFB_1-BSA (0.3 μL) at three different concentrations (0.75, 1, and 1.25 mg/mL) were

immobilized on the device. The BCIP/NBT substrate (0.6 μL), ALP-Ab, and sample were spotted on the device, before immersing the device into 70 μL of running buffer.

For the optimization of ALP-Ab concentration, the ALP-Ab zone was prepared with various concentrations of ALP-Ab (5, 10, 15, 20, and 25 μg/mL). The sample solutions (blank and 0.1 ng/mL AFB_1) were dropped on the ALP-Ab zones. Next, the device was dipped in the running buffer (70 μL). After finishing loading the buffer, the BCIP/NBT substrate (1.5 μL) was manually dropped into the detection channel on the device.

For selection of MeOH concentration in the running buffer, a simple experiment was carried out. MeOH was adjusted to various concentrations (0, 20, 40, 60, and 80%v/v) in the substrate buffer containing 0.1% (v/v) BSA. Protein precipitation was observed with the naked eye.

2.3.6 Automated detection of AFB_1

As shown in Figure 2.3.6, the sample solution containing AFB_1 antigen (0.3 μL each) was applied to the ALP-Ab zones on a ready-to-use device. The device was dipped in the running buffer (70 μL).

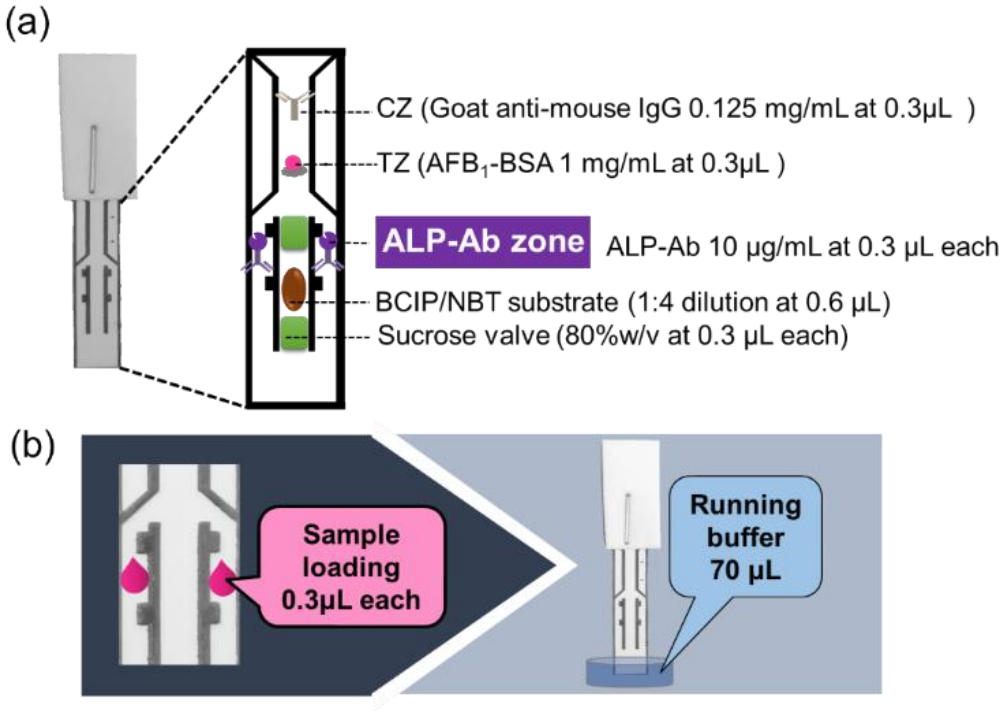

Figure 2.3.6 Automated detection of AFB_1. (a) A ready-to-use device with reagent location. (b) Sample loading-method.

2.3.7 Detection of spiked-AFB_1 soy sauce

The spiked-AFB_1 soy sauce (0.3 μL each) was applied to the ALP-Ab zones on the ready-to-use device, as shown in Figure 2.3.6. The device was immersed in the running buffer (70 μL).

2.4 Results and discussions

The initial sample-loading method was carried out following the original successful work of Apilux *et al*[1]. As shown in Figure 2.4.1., the device was dipped into 70 µL of sample solution containing AFB_1 at different concentration.

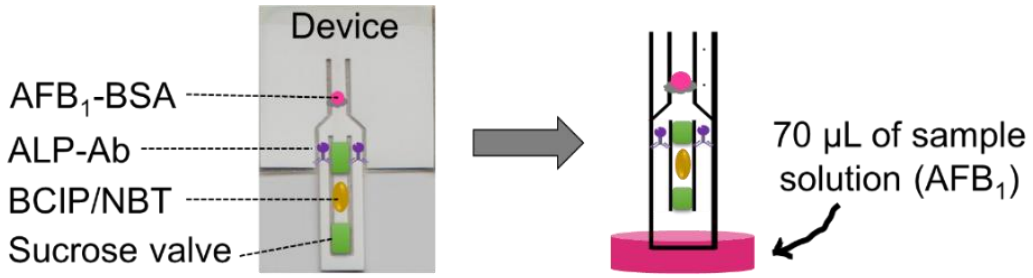

Figure 2.4.1. Device preparation and sample-loading method for automated detection of AFB_1. The device was prepared by AFB_1-BSA 1 mg/mL at 0.3 µL, ALP-Ab 25 µg/mL at 0.3 µL, BCIP/NBT substrates (1:2 dilution) at 0.6 µL, sucrose valve 80% w/v at 0.6 µL and solvent for sample dilution is 20% v/v ethanol in ALP buffer containing 0.001% BSA.

After the device was dipped into the sample solution, the automated sequential delivery of reagents occurred in three steps as shown in Figure 2.4.2.

- STEP 1: ALP-Ab (yellow dye) was delivered to the detection channel by capillary force
- STEP 2: the sucrose valve dissolved, therefore allowing the flow inside the middle channel
- STEP 3: BCIP/NBT (red dye) was released to the detection channel

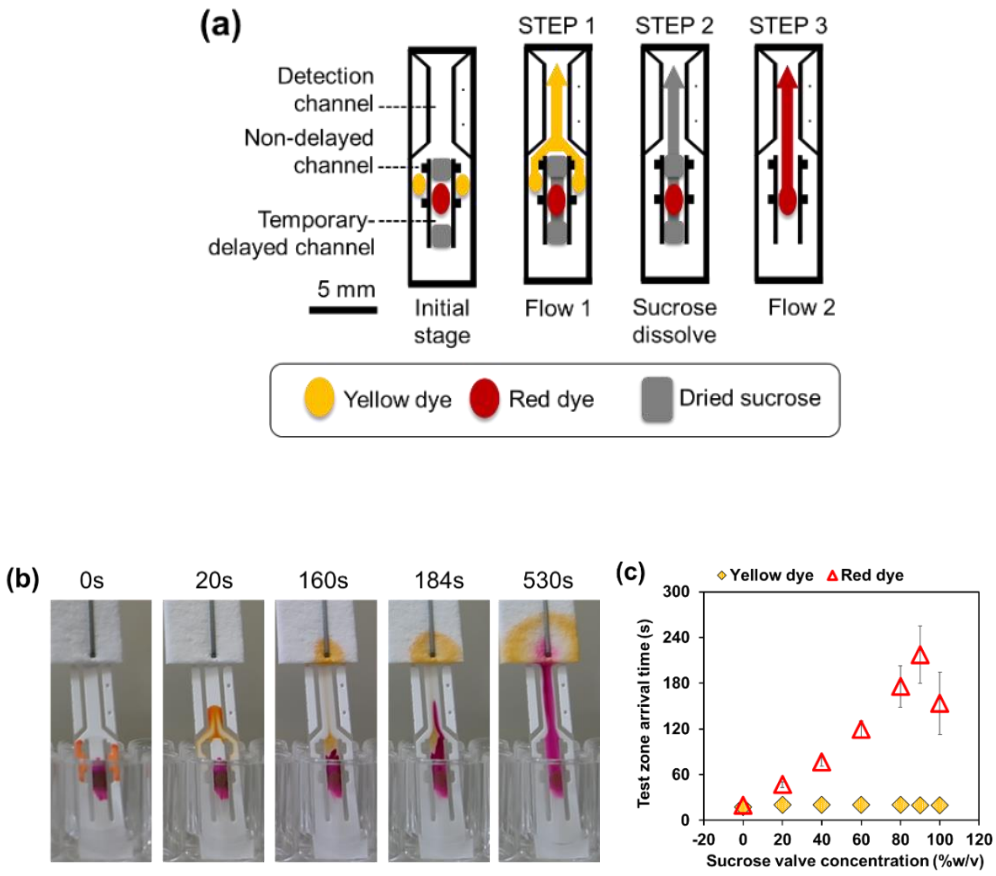

Figure 2.4.2 A sucrose valve on μPADs. (a) reagents delivery mechanism. (b) Images of a device prepared by 80% w/v sucrose valves. (c) Correlation between dyes delivery time and valve concentration (n=3).

The more delayed arrival time of reagent inside the middle channel (temporary delayed channel) could be achieved by adjusting the concentration of sucrose. This method allows simple control of sequential delivery of reagents without the need to change the physical pattern on the device.

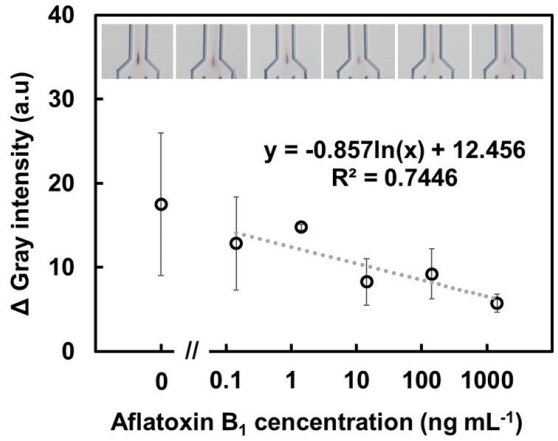

Figure 2.4.3. Detection of AFB_1. Images and plots of the mean color intensity of AFB_1 competitive ELISA (n=3).

The result from the automated detection of AFB_1 by this sample-loading method is shown in Figure 2.4.3. While the color intensity decreased in the 0 to 1,000 ng/mL samples, the high variation was observed. Moreover, the sensitivity of the detection was low, as shown by the standard curve fitted by logarithmic regressions with correlation coefficients (R^2 = 0.7446) for the concentration range of 0.1–1,000 ng/mL. Consequently, investigations into several parameters, e.g., device structure, sample-loading method, and reagent optimization, were important for increasing detection sensitivity.

2.4.1 Study of the device structure

To study the device structure, the number of device layers was investigated. Two different devices were fabricated to have 1 and 2 layers, as shown in Figure 2.4.1.1. The 1-layer device included reaction and absorbent areas on the NCM (Immunopore RP). The 2-layers device consisted of reaction pad (NCM, Immonopore RP) and the absorbent pad (cellulose fiber pad). Both 1-layer and 2-layers-devices were prepared by Anti-mouse IgG (Control zone, CZ) 0.125 mg/mL at 0.3 µL, AFB_1-BSA (Test zone, TZ) 1 mg/mL at 0.3 µL, ALP-Ab 25 µg/mL at 0.3 µL, BCIP/NBT substrates (1:2 dilution) at 0.6 µL, sucrose valve 80% w/v at 0.6 µL and solvent for sample dilution is 20% v/v ethanol in ALP buffer containing 0.001% BSA

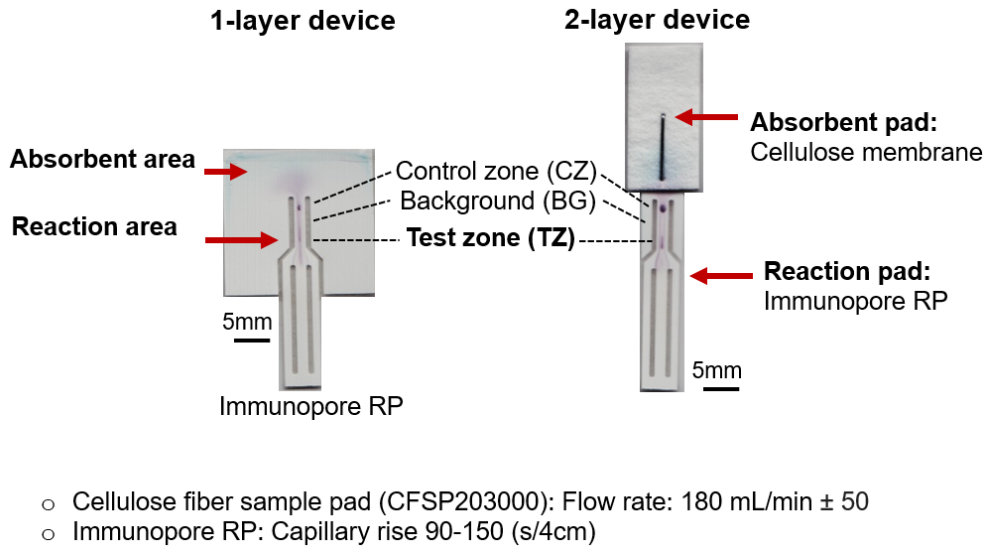

Figure 2.4.1.1. Structure of device.

The result of the intensity from the blank sample is shown in Figure 2.4.1.2. The 2-layer device shows a significant improvement in intensity at the test zone (TZ), making it clearly distinguishable from the background (BG). In addition, the decreasing of variation (error bar) was observed in the 2-layer device. These results could possibly be due to the use of a smaller size of absorbant pad while having more absorption capacity, which could provide more uniform flow and improved reaction efficiency. As a result, the 2-layers were chonsen for further experiments.

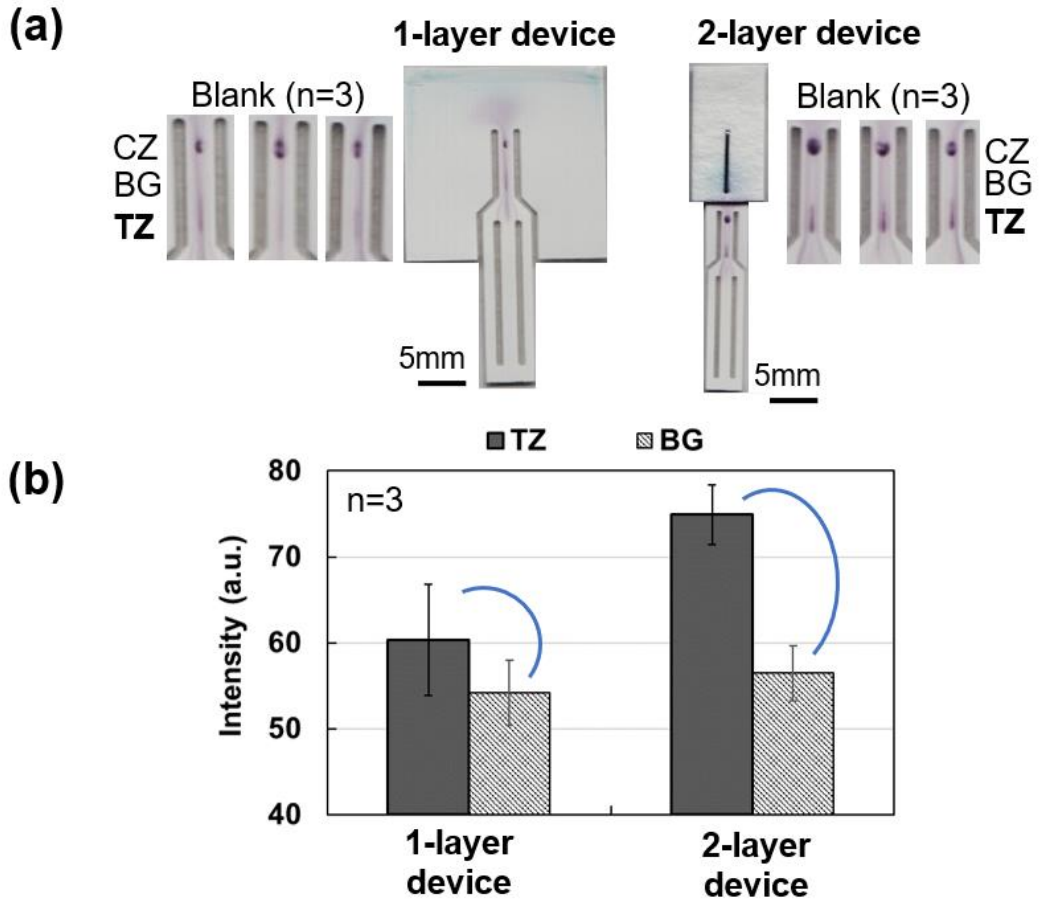

Figure 2.4.1.2. Effect of structure of device. (a) Image of devices. (b) The mean color intensity at blank sample (n=3).

2.4.2 Effect of sample-loading method

To investigate the effect of the sample-loading method, samples were loaded in three distinct locations: in a well plate (i), on the membrane below the ALP-Ab zones (ii), and at the ALP-Ab zones (iii), as shown in Figure 2.4.2.1 (a).

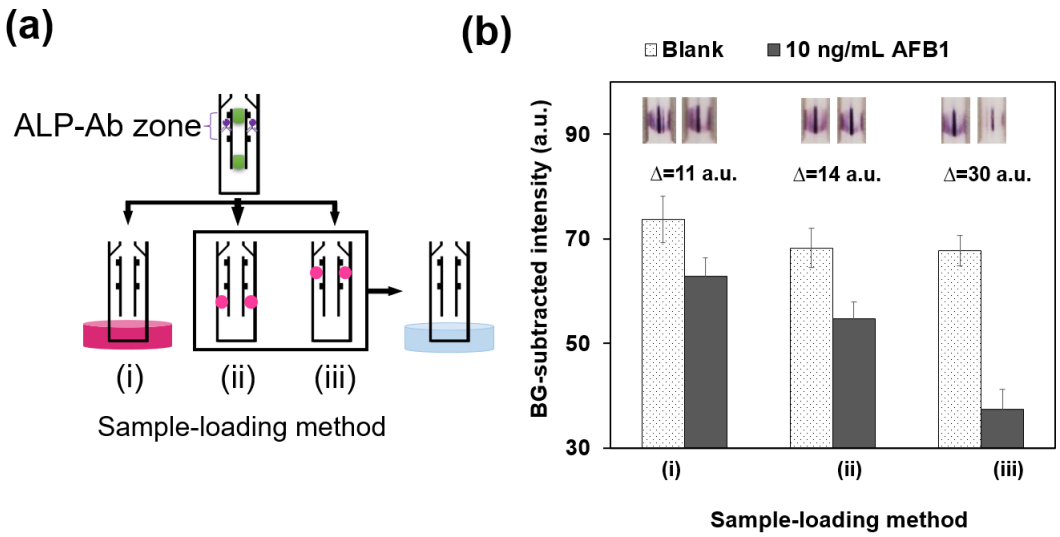

Figure 2.4.2.1 Effect of sample-loading method. (a) Experimental design. (b) Test zone (TZ) images and plots of the mean color intensity of AFB_1 competitive ELISA (n=3).

As shown in Figure 2.4.2.1 (b), when sample solution was placed into a well plate, the difference in intensity in the test zones between the blank and 10 ng/mL AFB_1 samples was very small (Δ=11 a.u.). Likewise, when sample solutions were dropped on the membrane at locations below the ALP-Ab zones, the difference in intensity at the device test zones between blank and 10 ng/mL AFB_1 samples was relatively small (Δ=14 a.u.). However, when sample solution was dropped on the

membrane directly in the ALP-Ab zones, the difference in intensity at the test zones between blank and 10 ng/mL AFB_1 samples was increased significantly (Δ=30 a.u.), suggesting improved reaction and sensitivity.

Due to sample losses during membrane transport, greater sample volumes are typically required to achieve improved sensitivity[15]. Interestingly, the results shown in Figure 2.4.2.1 demonstrated improved sensitivity and minimized sample volume simultaneously by using the same zones for ALP-Ab and sample loading.

To study the mechanism of high sensitivity in case (iii), sample solution (70 µL) was mixed with ALP-Ab (0.6 µL) in a well plate, as illustrated in Figure 2.4.2.2 (a)

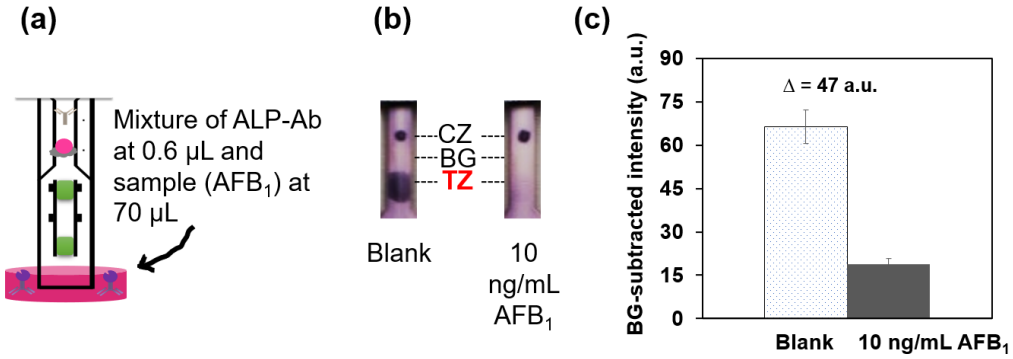

Figure 2.4.2.2 Direct mixing of the sample solution and ALP-Ab in a well plate. (a) experimental setup. (b) Test zone (TZ) images. (c) Plots of the mean color intensity of AFB_1 competitive ELISA (n=3).

As shown in Figure 2.4.2.2 (b), the signal at the test zones (TZ) between blank and 10 ng/mL AFB_1 samples was clearly visible to the naked eye. This difference in measured intensity (Δ=47 a.u.) was large, as demonstrated in Figure 2.4.2.2 (c), demonstrating a sufficient reaction in the well plate between AFB_1 and ALP-Ab.

In cases (i) and (ii), the insufficient reaction and low sensitivity could possibly be caused by a loss of the antigen sample due to adsorption on the membrane. Because AFB_1 is generally soluble in moderately polar organic solvents (e.g., methanol or chloroform) but scarcely soluble in water[16], some of the sample AFB_1 antigens may have become trapped on the membrane. These trapped AFB_1 molecules may not have been released, or the binding-site of AFB_1 was possibly hindered, preventing them from immunoreaction with antibodies at the ALP-Ab zones.

In case (iii), the sample solution was dropped directly into the Ab-ALP zones where antibodies were; therefore, AFB_1 was able to bind with antibodies immediately. Antibody binding may have increased the solubility of AFB_1 and reduced adsorption to the membrane. Consequently, the loss of the AFB_1 might have been suppressed.

To confirm the position accuracy required for sample dropping on the membrane, more sample dropping positions were examined. As depicted in Figure 2.4.2.3 (a), sample was dropped at 5 different locations (i-v), indicating the possibility of ALP-Ab and the sample overlapping in position. ALP-Ab (white

border) and sample positions (yellow dye) were, for example, completely overlapped by dropping the sample inside the ALP-Ab zone (i), partially overlapped (ii, iii), and totally separated by dropping the sample below (iv) and above (v) the ALP-Ab zone.

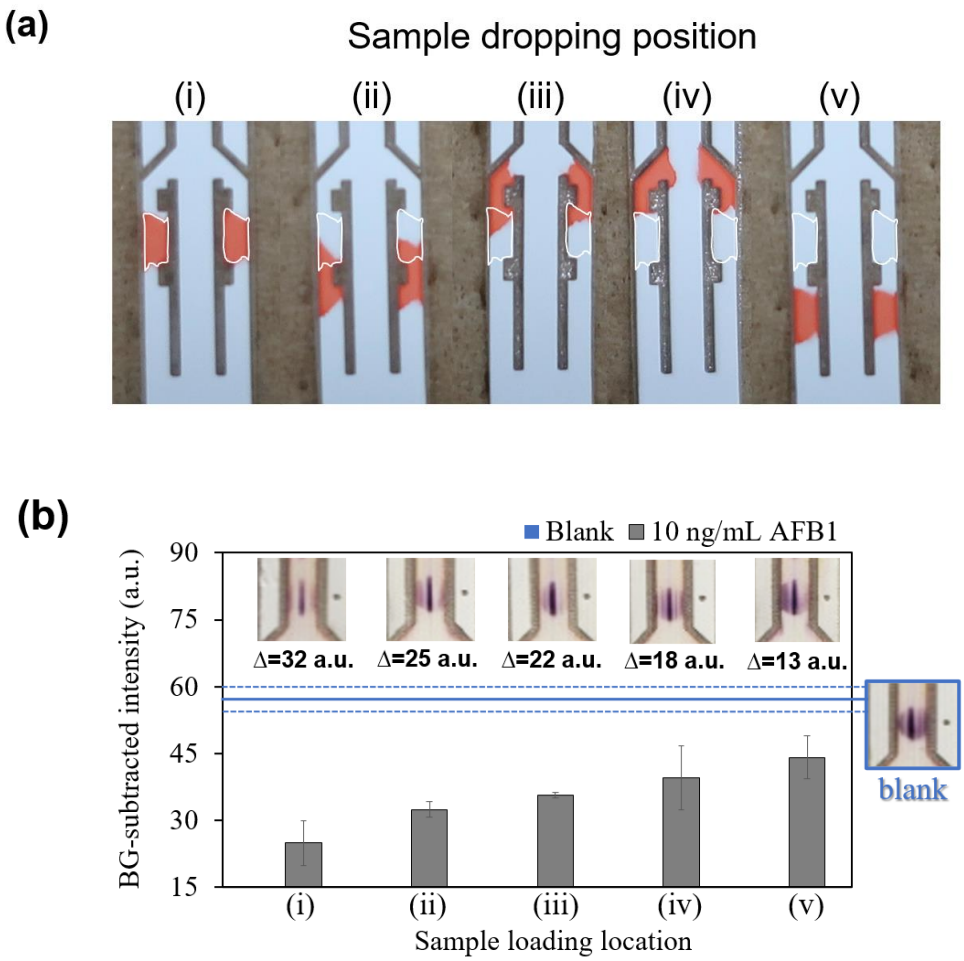

Figure 2.4.2.3 The effect of the sample dropping position. (a) Positional overlap of ALP-Ab (white borders) and sample (yellow dye). (b) Images of the test zone (TZ) and plots of the mean color intensity (n=3). The Δ value represents the mean intensity difference between the blank and 10 ng/mL AFB_1 samples.

As shown in Figure 2.4.2.3 (b), the difference in intensity in the test zones was the largest (=32 a.u.) when the ALP-Ab and sample positions were completely overlapped (i). The largest difference in intensity demonstrates the most sufficient position for improving reaction. This result confirms that by only using the same zones of the ALP-Ab for sample loading, improved reaction and sensitivity were achieved, without any changes to the reaction components or structural design of the devices. Therefore, we named this new sample-loading method as Direct Dropping of Sample on Antibody Location (DDoAb). DDoAb was then used for further experiments for AFB_1 Detection.

2.4.3 Optimization of reagents

Since the concentration of reagents, e.g., AFB_1-BSA, ALP-Ab, and Methanol (MeOH) in the running buffer affects the sensitivity and the limit of detection (LOD) of the detection, optimization of these reagents is necessary.

To optimize test zone conditions, both the volume and concentration of AFB_1-BSA were investigated. For volume optimization, three different volumes (0.3, 0.6, and 1.2 µL) of AFB_1-BSA (1.5 mg/mL) were immobilized on the devices. As shown in Figure 2.4.3.1 (a, b), the signal intensity and variation in both samples (blank and 10 ng/mL AFB_1) were high when the volume of AFB_1-BSA was increased to 0.6 and 1.2 µL. Because of the reproducibility aspect, 0.3 µL was then chosen as the optimal volume for the test zone immobilization.

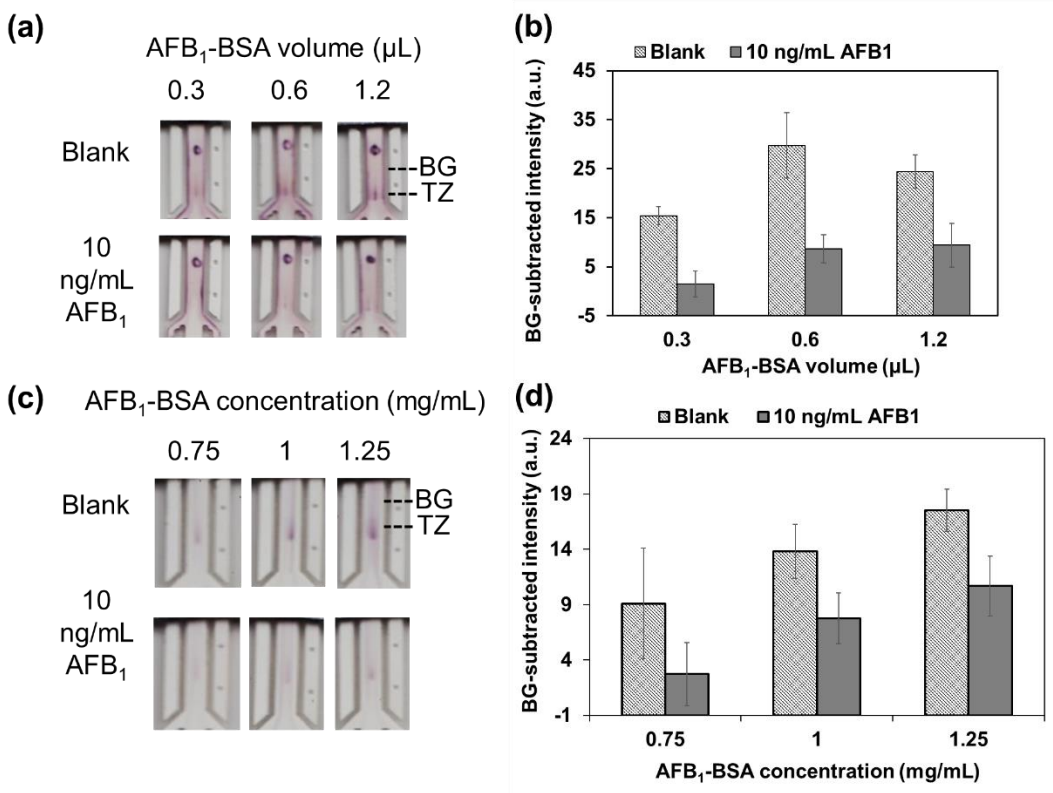

Figure 2.4.3.1 Test zone (AFB_1-BSA) optimization. (a, b) Volume and (c, d) concentration optimization for AFB_1-BSA.

To optimize the concentration of the test zone, AFB_1-BSA (0.3 µL) at three different concentrations (0.75, 1, and 1.25 mg/mL) were immobilized on the device. The results are shown in Figure 2.4.3.1 (c, d). Using automated delivery of the BCIP/NBT substrate, the signal intensity in both samples (blank and 10 ng/mL AFB_1) was low, while the variation was high when 0.75 mg/mL AFB_1-BSA was used as the test zone. The signal intensity response and variation were similar in the test zones of 1 and 1.25 mg/mL AFB_1-BSA. As a result, AFB_1-BSA at 1 mg/mL was chosen as the optimal concentration for the test zone.

Next, the optimization of concentrations of ALP-Ab was carried out. Several concentrations of 5, 10, 15, 20, and 25 μg/mL ALP-Ab were examined. As demonstrated in Figure 2.4.3.2, a concentration of 10 μg/mL ALP-Ab showed the largest difference in color intensity in the test zone between the blank and 0.1 ng/mL, suggesting the highest sensitivity for competitive ELISA of AFB_1. As a result, 10 μg/mL was selected as the optimal concentration for ALP-Ab.

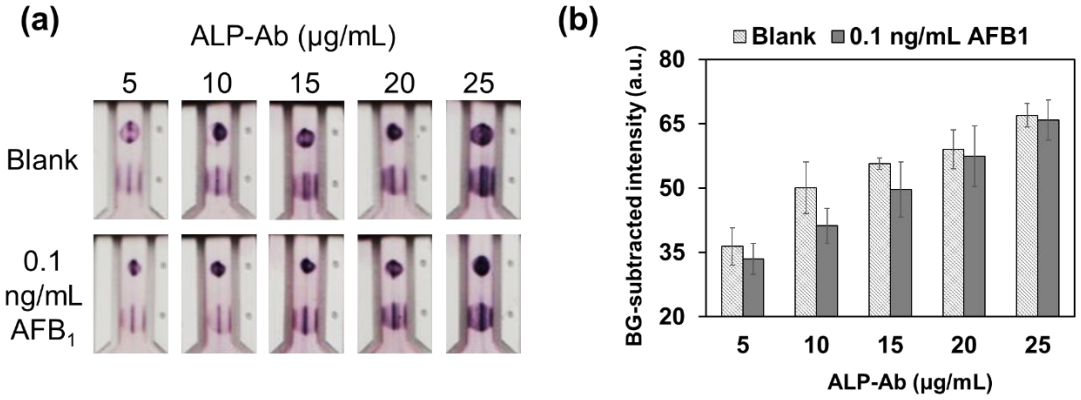

Figure 2.4.3.2 Antibody optimization. (a) Images of the paper-based device and (b) plots of the mean color intensity of the AFB_1 competitive ELISA at 0.1 ng/mL (n=3), using different antibody concentrations.

The running buffer in this system consists of three main components of chemicals. The first one is an alkaline buffer containing Tris and magnesium chloride for enzymatic reaction. The BSA molecule is the second component, which is typically employed to prevent antigen absorption into the sample tube or onto the membrane[17]. The third is MeOH, which assists in AFB_1 antigen solubility. Although a high concentration of MeOH is generally beneficial for

dissolving AFB_1 antigen, it can also cause a significant effect on overall performance in ELISA [18, 19]. Furthermore, MeOH can disrupt the structure of protein[20], including the BSA molecule in the running buffer. Thus, the appropriate concentration of MeOH for the assay was necessary. To select MeOH concentration for the running buffer, a simple experiment was conducted. In the running buffer containing 1% BSA, the concentration of MeOH was varied from 0 to 20, 40, 60, and 80 %v/v. As shown in Figure 2.4.3.3, protein precipitation was noticeable to the naked eye when the concentration of MeOH was higher than 40% v/v. As a result, 20% v/v MeOH was selected as the optimal running buffer concentration.

Figure 2.4.3.3 Methanol (MeOH) concentration (0-80% v/v) in the running buffer.

2.4.4 Automated detection of AFB_1

Automated competitive ELISA for the determination of AFB_1 was carried out using the DDoAb method under optimal condition. The standard AFB_1 sample solutions (0–10,000 ng/mL) were loaded to the ALP-Ab zones. Figure 2.4.4.1 (a) illustrates the results of the automated detection of AFB_1.

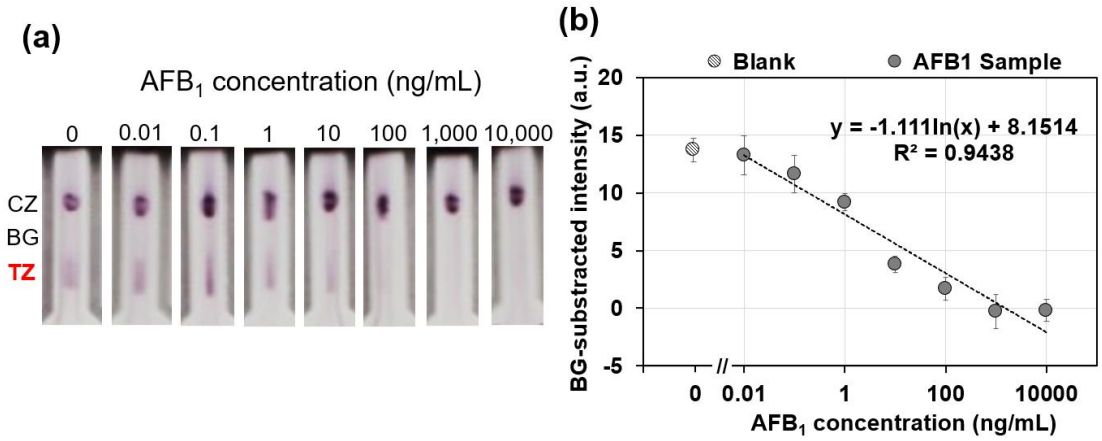

Figure 2.4.4.1 Automated competitive ELISA for the determination of AFB_1 by the DDoAb (a) Images of the paper-based devices and (b) the calibration curve of AFB_1 competitive ELISA from 0 to 10,00 ng/mL (n=3) using automated delivery of reagents by a sucrose valve at 80 % w/v.

The most significant color intensity change occurred at the test zone with the blank, 0.01 and 0.1 ng/mL samples. The color intensity decreased in the 1 to 10,000 ng/mL samples. The standard curve was fitted to logarithmic regressions with correlation coefficients (R^2 = 0.9438) for the concentration range of 0.01–10,000 ng/mL, as shown in Figure 2.4.4.1 (b). Based on the concentration

equivalent to the mean of the blank sample minus the triple standard deviation, the LOD was calculated to be 0.1 ng/mL. This LOD is 50 times lower than common regulatory limits of AFB_1 in foods and/or animal feed [21].

The lowest detectable amount of AFB_1 was calculated to be 60 femtograms, based on a sample volume of 0.6 μL and an LOD of 0.1 ng/mL. Table 2.4 shows that the femtogram level sensitivity of this device using the DDoAb method is 2-4 orders of magnitude lower than that of other AFB_1 paper-based devices.

Table 2.4 Comparison of paper-based devices for AFB_1 detection.

Ref	Detection method	User-operation	Sample (μL)	LOD (ng/mL)	LOD (g)
[22]	Enzyme-catalyzed chemiluminescence	Multi-step	50	0.15	7.5×10^{-12}
[23]	Fluorescent microspheres probe	2-step	100	2.5	2.5×10^{-10}
[24]	Colorimetric	1-step	100	0.25	2.5×10^{-11}
[25]	Colorimetric	Multi-step	20	9.45	1.89×10^{-10}
[8]	Colorimetric ELISA	2-step	50	1.31	6.55×10^{-11}
This work	Colorimetric ELISA	2-step	0.6	0.1	6.0×10^{-14}

Multi-step, three or more steps-manual operation.

2.4.5 Detection of spiked-AFB_1 soy sauce

To demonstrate the performance of the device in a real sample matrix, a measurement in Japanese soy sauce was chosen for several reasons. Firstly, soy sauces are made from fermented soybeans, which is one of the agricultural products that can be contaminated with AFB_1. Secondly, soy sauce is one of the most frequently consumed ingredients in daily life in many countries worldwide. Especially in Japan, soy sauce is often eaten raw as a seasoning with sushi and raw fish. Other dishes may have soy sauce cooked before eating. However, AFB_1 has highly resistant to heat, which has a decomposing temperature higher than 235 ◦C[26], and therefore there is still a chance of having AFB_1 remain contaminated after cooking. Lastly, soy sauce is a sample with a dark color. Often, samples with a dark color require pretreatment to eliminate the color, which could interfere with colorimetric detection. Our device requires an extremely low-sample volume (0.6μL) which can be beneficial for dark-colored samples.

Figure 2.4.5.1 illustrates the procedure for detection of AFB_1-spiked soy sauce. The soy sauce was manually contaminated by AFB_1 with known concentrations.

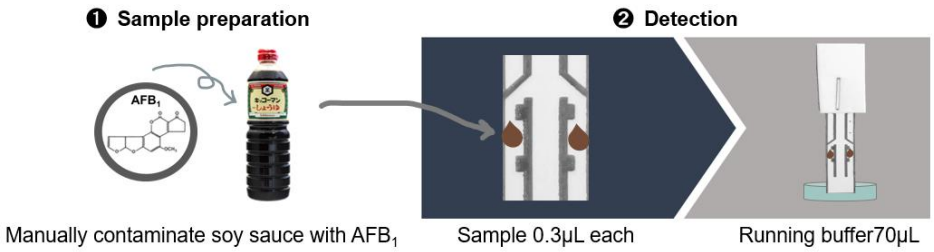

Figure 2.4.5.1 Procedure for detection of AFB_1-spiked soy sauce.

Without any pretreatment to the AFB_1-spiked soy sauce, the samples were loaded directly onto the device to perform the detection. Figure. 2.4.5.2 shows the calibration curve of spiked-AFB_1 in soy sauce. The LOD in soy sauce was calculated to be 4.8 ng/mL.

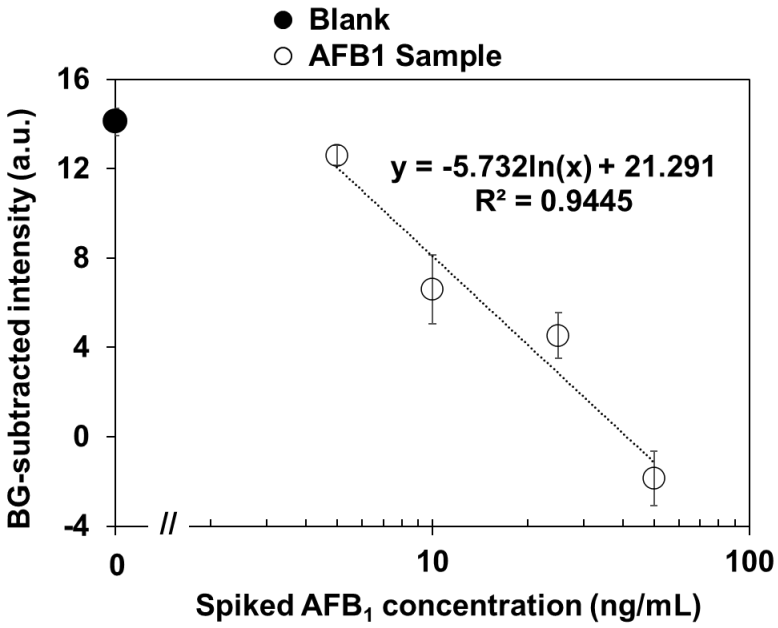

Figure 2.4.5.2 Real sample (AFB_1-spiked soy sauce) measurement. The calibration curve of spiked-AFB_1 in soy sauce from 0 to 50 ng/mL using automated delivery of reagents by a sucrose valve at 80% w/v (n=3).

2.5 Conclusion

a µPAD for automating the competitive ELISA was successfully developed for AFB_1 detection. Improved sensitivity while minimizing sample volume (0.6 µL) was achieved by using the DDoAb, a novel sample-loading method: dropping sample solution into the zones that had been prepared with an antibody-conjugated enzyme, followed by immersion in a running buffer. Under the optimal conditions, the device achieved a LOD of 0.1 ng/mL in the buffer matrix and 4.8 ng/mL in the soy sauce matrix. As a result, the proposed device provides high sensitivity, low cost, user-friendly, portability, and low volume sample measurement. This method could be used for a wide range of small-molecule detection applications, such as food safety, environmental monitoring, and clinical diagnosis. Especially in clinical diagnosis, the device can be used with a pinprick to collect blood samples in a very small volume (<1 µL), enabling more use of self-testing devices for biomarker detection in blood. Moreover, this method can be beneficial for difficult-to-obtain biological samples such as tears and brain fluids.

2.6 References

[1] A. Apilux, Y. Ukita, M. Chikae, O. Chailapakul, Y. Takamura, Development of automated paper-based devices for sequential multistep sandwich enzyme-linked immunosorbent assays using inkjet printing, Lab on a Chip, 13 (2013) 126-135.

[2] P. Preechakasedkit, W. Siangproh, N. Khongchareonporn, N. Ngamrojanavanich, O. Chailapakul, Development of an automated wax-printed paper-based lateral flow device for alpha-fetoprotein enzyme-linked immunosorbent assay, Biosensors and Bioelectronics, 102 (2018) 27-32.

[3] H. Fu, P. Song, Q. Wu, C. Zhao, P. Pan, X. Li, N.Y.K. Li-Jessen, X. Liu, A paper-based microfluidic platform with shape-memory-polymer-actuated fluid valves for automated multi-step immunoassays, Microsystems & Nanoengineering, 5 (2019) 50.

[4] Y. Wu, Y. Ren, L. Han, Y. Yan, H. Jiang, Three-dimensional paper based platform for automatically running multiple assays in a single step, Talanta, 200 (2019) 177-185.

[5] B. Gao, J. Chi, H. Liu, Z. Gu, Vertical Paper Analytical Devices Fabricated Using the Principles of Quilling and Kirigami, Scientific Reports, 7 (2017) 7255.

[6] Y.-T. Lai, C.-H. Tsai, J.-C. Hsu, Y.-W. Lu, Microfluidic Time-Delay Valve Mechanism on Paper-Based Devices for Automated Competitive ELISA, Micromachines, 10 (2019).

[7] T. Komatsu, Y. Sato, M. Maeki, A. Ishida, H. Tani, M. Tokeshi, Rapid, sensitive universal paper-based device enhances competitive immunoassays of small molecules, Analytica Chimica Acta, 1144 (2021) 85-95.

[8] L.S. Busa, S. Mohammadi, M. Maeki, A. Ishida, H. Tani, M. Tokeshi, A competitive immunoassay system for microfluidic paper-based analytical detection of small size molecules, Analyst, 141 (2016) 6598-6603.

[9] A.V. Gutierrez R, M. Hedström, B. Mattiasson, Screening of self-assembled monolayer for aflatoxin B1 detection using immune-capacitive sensor, Biotechnology Reports, 8 (2015) 144-151.

[10] C.G. Awuchi, E.N. Ondari, S. Nwozo, G.A. Odongo, I.J. Eseoghene, H. Twinomuhwezi, C.U. Ogbonna, A.K. Upadhyay, A.O. Adeleye, C.O.R. Okpala, Mycotoxins’ Toxicological Mechanisms Involving Humans, Livestock and Their Associated Health Concerns: A Review, Toxins, 14 (2022).

[11] S. Marchese, A. Polo, A. Ariano, S. Velotto, S. Costantini, L. Severino, Aflatoxin B1 and M1: Biological Properties and Their Involvement in Cancer Development, Toxins, 10 (2018) 214.

[12] D.K. Mahato, K.E. Lee, M. Kamle, S. Devi, K.N. Dewangan, P. Kumar, S.G. Kang, Aflatoxins in Food and Feed: An Overview on Prevalence, Detection and Control Strategies, Front Microbiol, 10 (2019).

[13] B. Lutz, T. Liang, E. Fu, S. Ramachandran, P. Kauffman, P. Yager, Dissolvable fluidic time delays for programming multi-step assays in instrument-free paper diagnostics, Lab Chip, 13 (2013) 2840-2847.

[14] I. Dojindo Molecular Technologies, Alkaline Phosphatase Labeling Kit-SH, in, 2014.

[15] M.P. Nguyen, N.A. Meredith, S.P. Kelly, C.S. Henry, Design considerations for reducing sample loss in microfluidic paper-based analytical devices, Analytica Chimica Acta, 1017 (2018) 20-25.

[16] S. Choochuay, J. Phakam, P. Jala, T. Maneeboon, N. Tansakul, Determination of Aflatoxin B1 in Feedstuffs without Clean-Up Step by High-Performance Liquid Chromatography, International Journal of Analytical Chemistry, 2018 (2018) 4650764.

[17] C.K. Dixit, S.K. Vashist, B.D. MacCraith, R. O'Kennedy, Evaluation of apparent non-specific protein loss due to adsorption on sample tube surfaces and/or altered immunogenicity, Analyst, 136 (2011) 1406-1411.

[18] M. Rehan, H. Younus, Effect of organic solvents on the conformation and interaction of catalase and anticatalase antibodies, International Journal of Biological Macromolecules, 38 (2006) 289-295.

[19] N.A. Lee, S. Rachmawati, A rapid ELISA for screening aflatoxin B1 in animal feed and feed ingredients in Indonesia, Food and Agricultural Immunology, 17 (2006) 91-104.

[20] Q. Shao, Y. Fan, L. Yang, Y.Q. Gao, From protein denaturant to protectant: comparative molecular dynamics study of alcohol/protein interactions, The Journal of chemical physics, 136 (2012) 115101.

[21] W.-B. Shim, K. Kim, J.A. Ofori, Y.-C. Chung, D.-H. Chung, Occurrence of Aflatoxins in Herbal Medicine Distributed in South Korea, Journal of Food Protection, 75 (2012) 1991-1999.

[22] M. Zangheri, F. Di Nardo, L. Anfossi, C. Giovannoli, C. Baggiani, A. Roda, M. Mirasoli, A multiplex chemiluminescent biosensor for type B-fumonisins and aflatoxin B1 quantitative detection in maize flour, Analyst, 140 (2015) 358-365.

[23] D. Liu, Y. Huang, M. Chen, S. Wang, K. Liu, W. Lai, Rapid detection method for aflatoxin B1 in soybean sauce based on fluorescent microspheres probe, Food Control, 50 (2015) 659-662.

[24] X. Li, P. Li, Q. Zhang, R. Li, W. Zhang, Z. Zhang, X. Ding, X. Tang, Multi-component immunochromatographic assay for simultaneous detection of aflatoxin B1, ochratoxin A and zearalenone in agro-food, Biosensors and Bioelectronics, 49 (2013) 426-432.

[25] X. Tang, R. Su, H. Luo, Y. Zhao, L. Feng, J. Chen, Colorimetric detection of Aflatoxin B1 by using smartphone-assisted microfluidic paper-based analytical devices, Food Control, 132 (2022) 108497.

[26] P. Sipos, F. Peles, D.L. Brassó, B. Béri, T. Pusztahelyi, I. Pócsi, Z. Győri, Physical and Chemical Methods for Reduction in Aflatoxin Content of Feed and Food, Toxins, 13 (2021).

CHAPTER III

DIGITAL COUNTING ENZYNMATIC-µPAD

A digital counting of molecules is demonstrated on a colorimetric enzymatic- µPAD. To address the complexity and high cost of the use of microarrays in conventional digital enzyme-linked immunosorbent assays (ELISA), a simple enzymatic reaction that produced an insoluble color product was used for direct localization of the molecule and its amplified signal as dots on µPAD.

To amplify the signal for visualization, the µPAD was kept moistened in a plastic box, allowing for sufficient incubation for the enzymatic reaction and signal (dots) production. The presence of individual visible dots indicated the presence of molecules. The effect of incubation time on dot production is investigated in this study. The sensitivity of µPAD at the single-molecule level was demonstrated by digitally counting visible dots in microscopic images using software processing. Preliminary results showed that this proposed method successfully counts streptavidin-conjugated alkaline phosphatase (SA-ALP) molecules digitally at the picogram level (pg/mL), utilizing inexpensive materials and general laboratory equipment.

3.1 Introduction

Increasing the sensitivity of biosensors provides numerous advantages for bioanalytical applications. These advantages include improved health outcomes

and survival rates, particularly for early-stage cancer monitoring, which could facilitate diagnosis and treatment [1]. Since the amounts of disease-related proteins in biofluid samples can be as low as single or countable biomarker molecules, early disease diagnostics necessitate highly sensitive protein detection[2]. As a result, the development of a new analytical approach sensitive enough to detect biomarkers at the single-molecule level is crucial.

Previously, our group developed intensity-based inkjet-printed µPADs for automating a sandwich-type ELISA for human chorionic gonadotropin levels (hCG)[3]. More recently, the automated detection of Aflatoxin B_1 on µPAD using a competitive-type ELISA was achieved with a limit of detection (LOD) of 0.1 ng/mL[4]. Both devices depended on analog counting based on signal intensity, as shown in Figure 3.1. The signal was insoluble color products from an alkaline phosphatase (ALP) reaction.

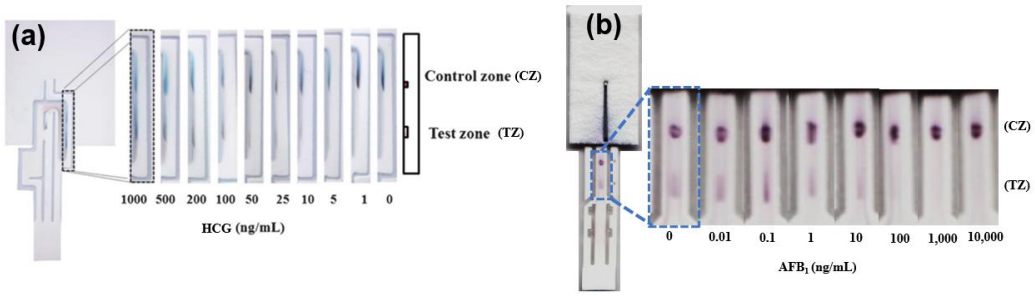

Figure 3.1 Analog counting ELISA-µPADs using insoluble color products from an alkaline phosphatase (ALP) reaction. (a) Sandwich-ELISA µPAD for HCG detection. Adapted with permission from ref. 3. Copyright © 2013 Royal Society of Chemistry. (b) Competitive-ELISA µPAD for AFB_1 detection.

Although the analog counting on µPADs was simple and straightforward, the absolute amount of signal can be hindered by noise, which may lead to undetectable results at low sample concentrations. As a result, increasing colorimetric µPAD sensitivity to the single-molecule detection level remains a challenge.

Several studies have shown the versatility of digital ELISA for single molecule detection by utilizing femtoliter-sized reaction chambers[5-7]. These small chambers play important role as to compartmentalize individual molecule and confine its signal which is a fluorescent color produced by the enzymatic reaction. As a result, the detection of single immunocomplex could be done by counting the presence of signals from each chamber[8]. Although the digital ELISA inside the small chamber allows the localization and detection of single enzyme molecules, this detection platform requires both complexity and special instruments which are not portable and thus impractical where affordability and simplicity are essential.

In this chapter, we demonstrate single-molecule detection without the use of an ultra-small chamber before digital counting on a µPAD for. As a proof of concept, the detection of streptavidin-conjugated alkaline phosphatase (SA-ALP) was carried out.

3.2 Objective

The objective of this study is to develop a method for digital counting on µPAD. As a proof of concept, streptavidin-conjugated alkaline phosphatase (SA-

ALP) molecules were digitally counted on μPAD through microscopic image. A study on incubation time for signal production is presented.

3.3 Experimental

The following is a list of the chemicals, materials, and equipment used in this study, as well as information on reagent preparation, μPADs fabrication, and the detection method.

3.3.1 Chemicals, materials, and equipment

Analytical-grade reagents and 18 MΩ-cm resistance water (obtained from a Barnstrad Milli-Q purification system). Other chemicals are listed in Table 3.1.

Table 3.1 List of chemicals.

Chemicals	Suppliers
The BCIP/NBT (5- bromo-4-chloro-39-indolyphosphate p-toluidine salt, nitro-blue tetrazolium chloride) substrate solution	Nacalai Tesque (Kyoto, Japan)
Substrate buffer solution	Nacalai Tesque (Kyoto, Japan)
Streptavidin conjugated-alkaline phosphatase (SA-ALP)	Sigma-Aldrich (Tokyo, Japan)
Albumin biotin labeled bovine (biotin-BSA)	Sigma-Aldrich (Tokyo, Japan)

Chemicals	Suppliers
Tris-HCl buffer solution 0.05 M pH 7.6	Wako (Japan)
Boric acid	Wako (Japan)
Casein	Wako (Japan)
Polyoxyethylene (20) sorbitan monolaurate (Tween 20)	Wako (Japan)
Tris(hydroxymethyl)aminomethane	Wako (Japan)
Sodium hydroxide	Wako (Japan)

The list of materials, equipment and suppliers that were used throughout the experiments is shown in Table 3.2.

Table 3.2 List of materials and equipment.

Equipment	Suppliers
Soft tissue paper, delicate Task Wipers	Kimwires (Japan)
Plastic box (PS Case No.4)	AS ONE Corporation (Osaka, Japan)
Digital HF microscope (VH8000C)	Keyence (Japan)
Nitrocellulose membrane, immunopore RP, capillary flow 90-150 sec/4 cm, code number 78356403	GE Healthcare (Japan)
Absorbent pad, code number CFSP203000	EMD Millipore Corporation

Equipment	Suppliers
Laser machine, VLS 3.50	Universal Laser Systems (Scottsdale, AZ, USA)
Laptop Computer, ThinkPad X240	Lenovo (Japan)
ImageJ software	National Institutes of Health (Bethesda, MD, USA)
Digital hotplate/stirrer PMC 720	Barnstead Thermolyne Corporation
Oven, DKN301	Yamato (Japan)
pH meter, F-72 LAQUA	Horiba Scientific
Desktop scanner, LiDE 220	Canon Inc. (Japan)

3.3.2 Reagent preparation

The details of reagent preparation are listed as follows:

- **The blocking solution** was 1% (w/v) casein in milk in 50 mM boric acid buffer.
- **The washing solution** was 20 mM Tris-HCl buffer (pH 7.6) with 0.1 % (v/v) Tween.
- **The test zone (TZ)** was prepared at 0.5 mg/mL of biotin-BSA in 0.05 M Tris-HCl buffer pH 7.6.

- **The BCIP/NBT substrate** was prepared by diluting the commercial BCIP/NBT with the substrate buffer (which is a Tris-HCl buffer solution containing Magnesium Chloride) at a ratio of 1:4.
- **Streptavidin conjugated-alkaline phosphatase (SA-ALP)** was prepared by dilution in 0.05 M Tris-HCl buffer containing 1% BSA to the desired concentration.

3.3.3 Fabrication of µPAD

The pattern of µPAD was designed using CorelDRAW, and the nitrocellulose membrane (NCM) was cut by laser. The membrane was then cleaned by dipping in water for 30 minutes and drying at 37 °C for 30 min. The test zone of the device was prepared by spotting 0.3 µL of 0.5 mg/mL of biotin-BSA 0.05 M Tris-HCl buffer on the membrane. After drying for 30 min at room temperature, the membrane was treated with blocking (1% w/v casein in milk in 50 mM boric acid buffer) and washing solution (0.1 % Tween 20) for 30 min each at room temperature before drying at 37 °C for 2 h. The absorbent pad was simply attached to the membrane using a regular office stapler.

3.3.4 Detection of Streptavidin

The device was dipped into a mixture of 0.6 µL of SA-ALP (prepared by dilution of SA-ALP with 0.05 M Tris-HCl buffer containing 1% BSA) and 70 µL of substrate buffer. After finishing solution loading, the device was cut to keep only the detection zone. The BCIP/NBT substrate (1:4 dilution) at 2.5 µL was dropped

onto the detection zone before being put in the moist plastic box (prepared by attaching wet-soft tissue paper to the plastic box) and being placed in the incubator at 25 °C for 48h. The membrane was dried at room temperature followed by images capture using a desktop scanner that operated at -50 brightness and +20 contrast and digital HF microscope.

3.3.5 Data analysis

For digital counting, images from the microscope were used to count the number of dots by ImageJ software, as shown in Figure 3.3.5.

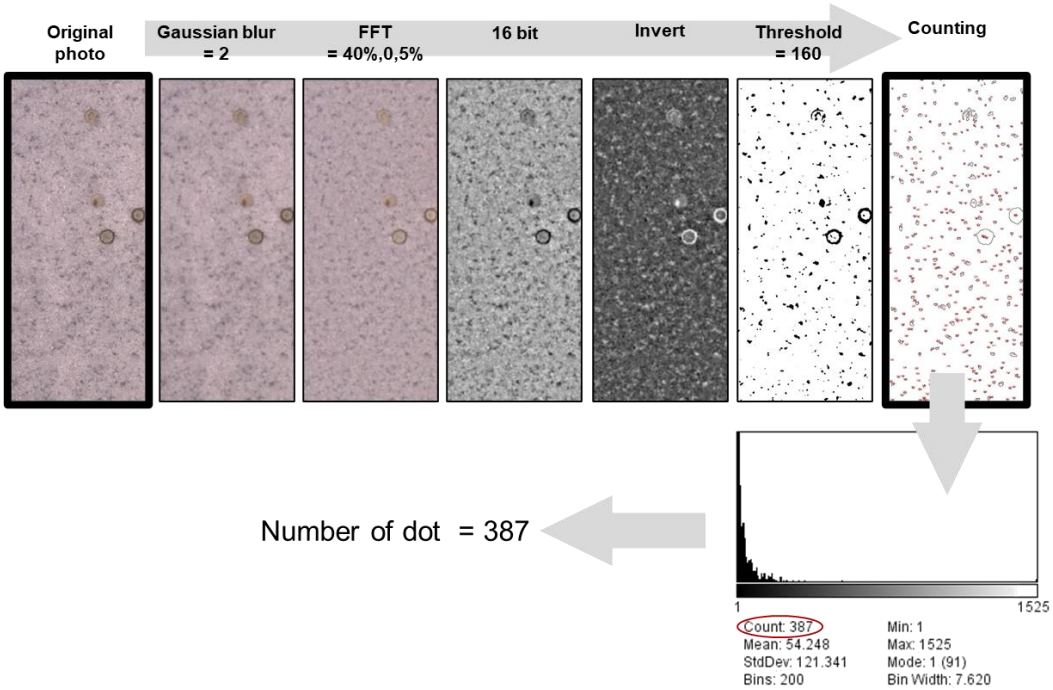

Figure 3.3.5 Data processing on Image J software for digital counting of signal (dot).

3.4 Results and discussions

3.4.1 The principle of digital counting on a µPAD for single-molecule detection

In this work, an insoluble purple color product from an alkaline phosphatase (ALP) reaction was used as a signal to identify the present of streptavidin-conjugated alkaline phosphatase (SA-ALP) molecules. Instead of using magnetic beads and femtoliter-sized chambers for localization of molecules, laser-cut nitrocellulose membrane (NCM) was used as the main material for the µPAD.

The detailed principle of a µPAD for digital counting of SA-ALP molecules is shown in Figure 3.4.1. Biotin-BSA was immobilized as a test zone on µPAD by physical absorption. The membrane was treated with blocking solution to prevent non-specific binding. The test zone was designed to be the smallest part of the device to minimize the volume of reagents and facilitate the flow to the absorbent pad. After a sample solution containing SA-ALP was loaded to the device, SA-ALP molecules were driven vertically through the test zone by capillary force. SA has an extremely high affinity for biotin[9], therefore SA-ALP molecules are bond to biotin at the test zone, forming a SA-biotin-SA-ALP complex at the test zone. To visualize SA molecules, an enzymatic reaction between ALP and BCIP/NBT was used to produce insoluble purple color product as a signal. The ALP enzyme, which was conjugated with SA, hydrolyzed BCIP to from a blue intermediate[10]. This intermediate was further oxidized by NBT to produce a dimer, which was an intense insoluble purple dye. This reaction was inside the moist plastic box to prevent the evaporation of reagents. The visible dots at the test zone from microscopic image

indicated the present of enzymatic reaction and SA-ALP molecule. The number of SA-ALP molecules was counted digitally through the number of visible dots on microscopic images using ImageJ software.

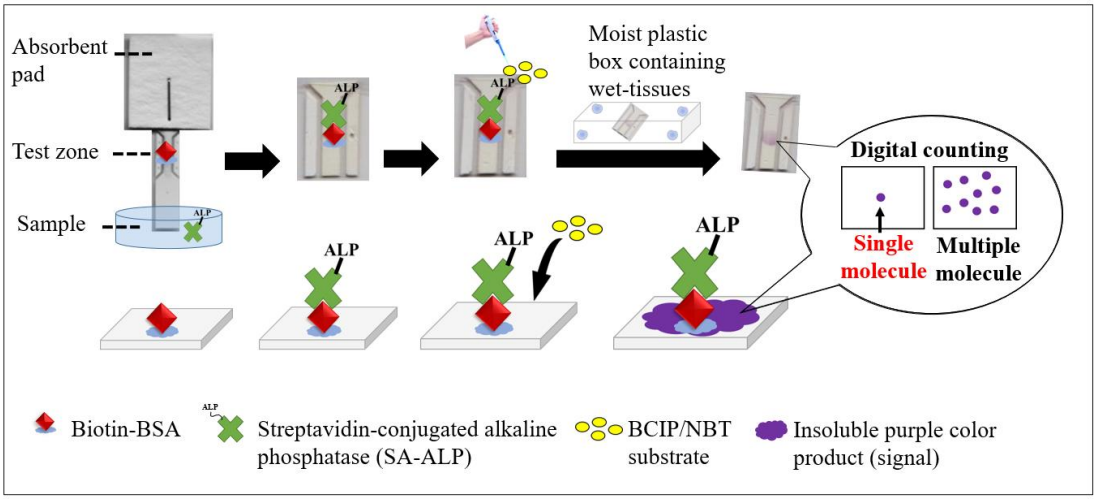

Figure 3.4.1 Schematic illustration of a µPAD for digital counting of SA-ALP molecules.

3.4.2 Optimization of the conditions for enzymatic reaction

As the amount of insoluble purple color or signal production depends on the incubation time of enzymatic reaction, it is necessary to allow sufficient incubation time to continue producing the signal until it appears as a dot. In order to demonstrate the effect of incubation time to the signal production, the test zone of µPAD was incubated at different incubation time (0-480 min). The test zone at 0.3 µL of 0.5 mg/mL biotin-BSA, 70 µL of 0.85 ng/mL SA-ALP containing 0.1% v/v BSA in substrate buffer and 2.5 µL of BCIP/NBT substrate (1:4 dilution) were used.

The images of the devices and the increase in intensity (analog counting) with incubation time are shown in Figure 3.4.2.1. Microscopic imaging of visible dark dots of amplified signals from SA-ALP molecules (digital counting) is shown in Figure 3.4.2.2. Longer incubation time resulted in an increased number of visible dots because one ALP molecule can hydrolyze many BCIP molecules[11], and thus allows more production of insoluble purple color product.

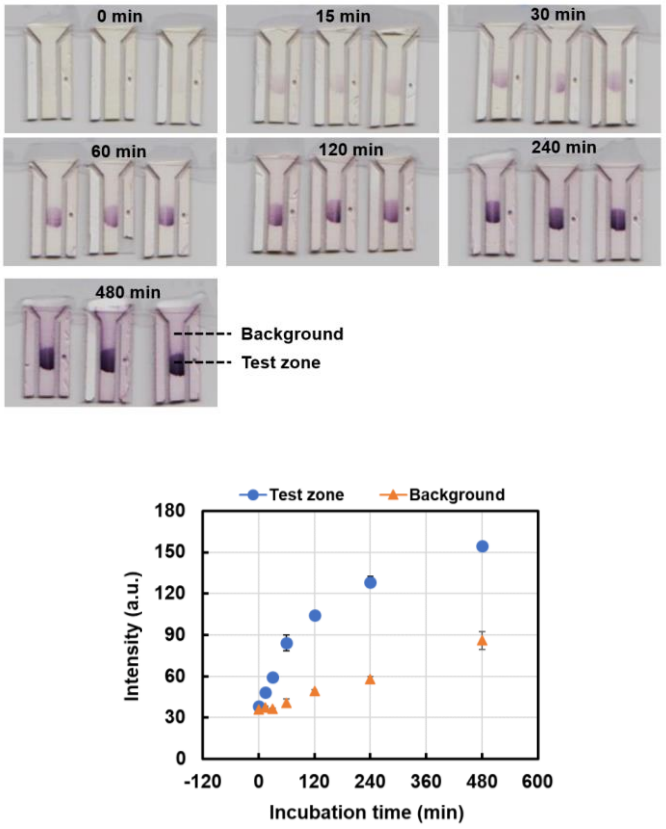

Figure 3.4.2.1 Analog counting. Images of the test zone of µPADs with different incubation times (0-480 min) under the condition at the test zone of 0.3 µL at 0.5 mg/mL biotin-BSA, 70 µL of 0.85 ng/mL SA-ALP containing 0.1% v/v BSA in substrate buffer and 2.5 µL of BCIP/NBT substrate (1:4 dilution) and the corresponding intensity response.

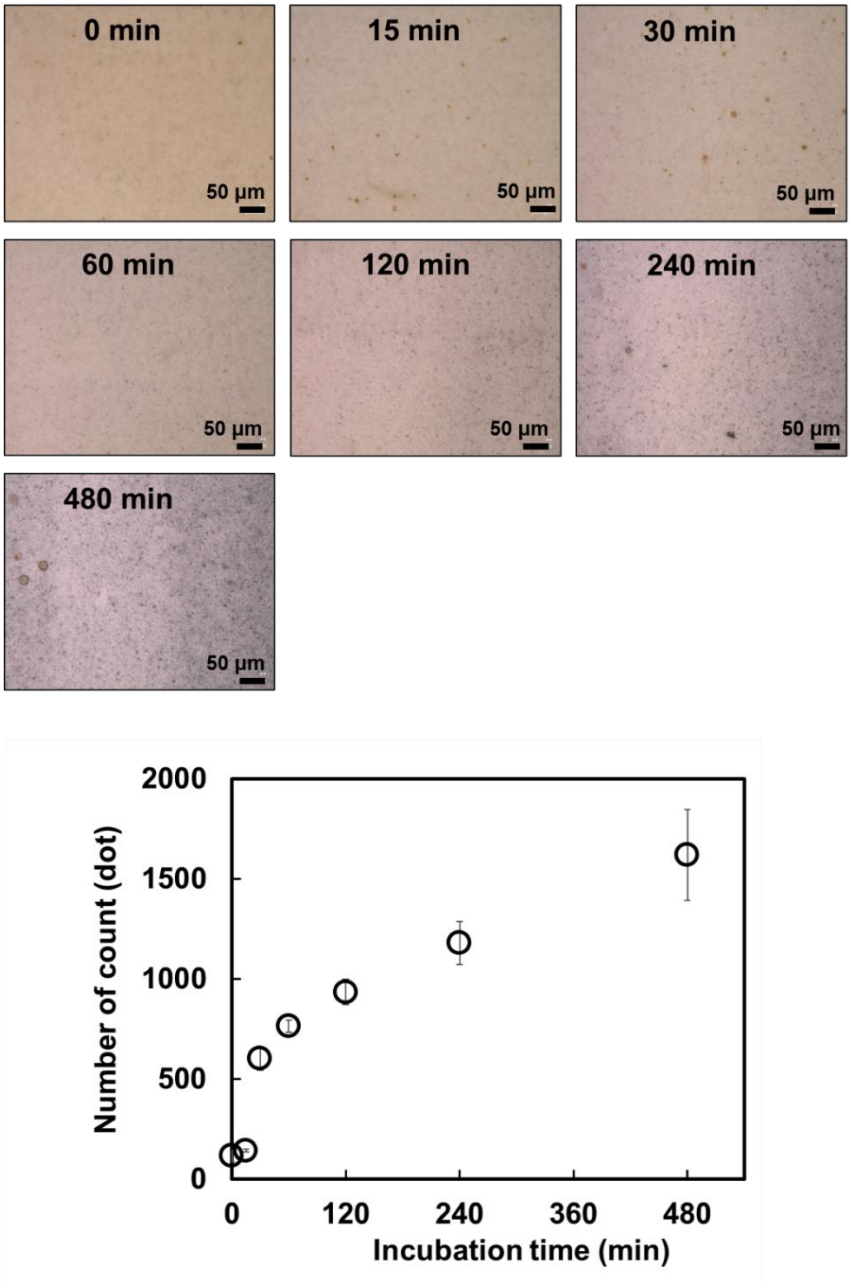

Figure 3.4.2.2 Digital counting. Microscopic images of the test zone of µPADs with different incubation times (0-480 min) under the condition at the test zone of 0.3 µL at 0.5 mg/mL biotin-BSA, 70 µL of 0.85 ng/mL SA-ALP containing 0.1% v/v BSA in substrate buffer and 2.5 µL of BCIP/NBT substrate (1:4 dilution) and the corresponding number of count (dot) response.

In order to obtain a higher sensitivity of SA-ALP detection, a better dot visualization of 85 pg/mL SA-ALP was done at much longer incubation time (48h). As expected, the number of amplified dots of signal from SA-ALP molecule increased from 23±14 dots at 0h to 1,946±97 dots at 48h incubation on µPADs as shown in Figure 3.4.2.2.

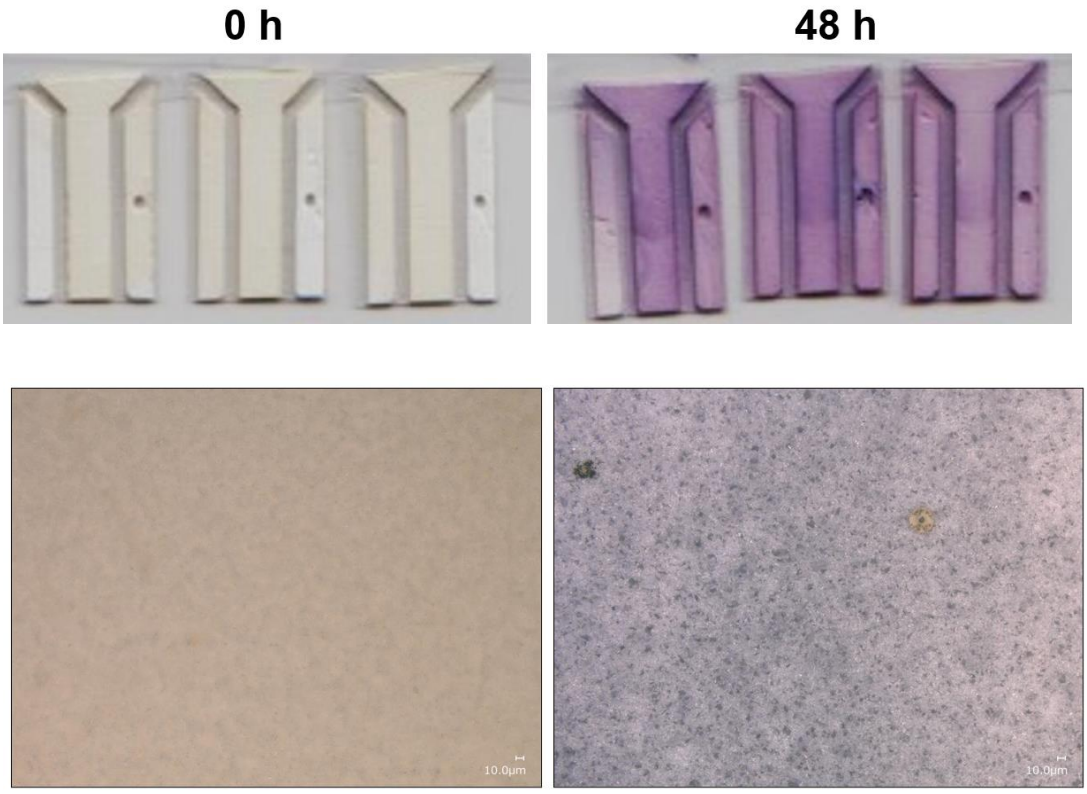

Figure 3.4.2.2 Microscopic images of the test zone of µPADs at 0 and 48 h incubation under the condition at the test zone of 0.3 µL at 0.5 mg/mL biotin-BSA, 70 µL of 85 pg/mL SA-ALP containing 0.1% v/v BSA in substrate buffer and 2.5 µL of BCIP/NBT substrate (1:4 dilution).

3.4.3 Digital Counting on a µPAD for SA-ALP

In order to demonstrate the digital countability on µPADs for SA-ALP molecules, different concentrations of SA-ALP were incubated on µPAD at 48h. Images of the test zone of µPADs at different concentration of SA-ALP (0.85 to 850 pg/mL) is shown in Figure 3.4.3.1. The number of visible dots correlated to the concentration of SA-ALP is shown in Figure 3.4.3.2. At low concentration of SA-ALP (0.85 pg/mL), fewer ALP molecules reacted with BCIP/NBT substrate and leaded to lower production of insoluble purple color product as visible dots at the given 48 h incubation. Without the use of femtoliter-sized chambers, single-molecule level detection as low as 0.85 pg/mL of SA-ALP was successfully conducted using inexpensive materials and general laboratory equipment, e.g., nitrocellulose membrane, plastic box, paper tissue, pipette, incubator and microscope. This simple-highly sensitive detection platform shows potential for use in other bioanalytical applications and other target molecules.

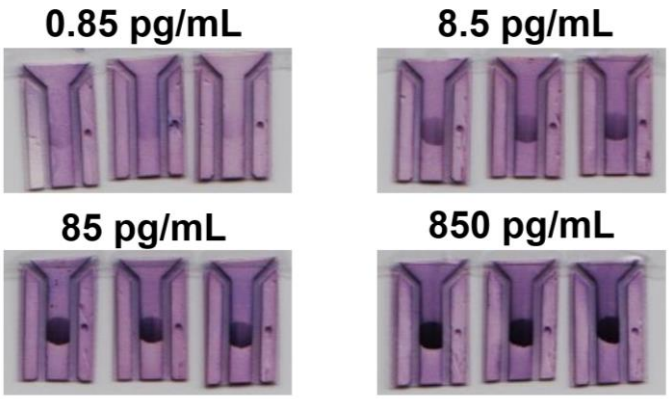

Figure 3.4.3.1 Images of the test zone of µPADs at different concentration of SA-ALP (0.85 to 850 pg/mL) after 48h incubation.

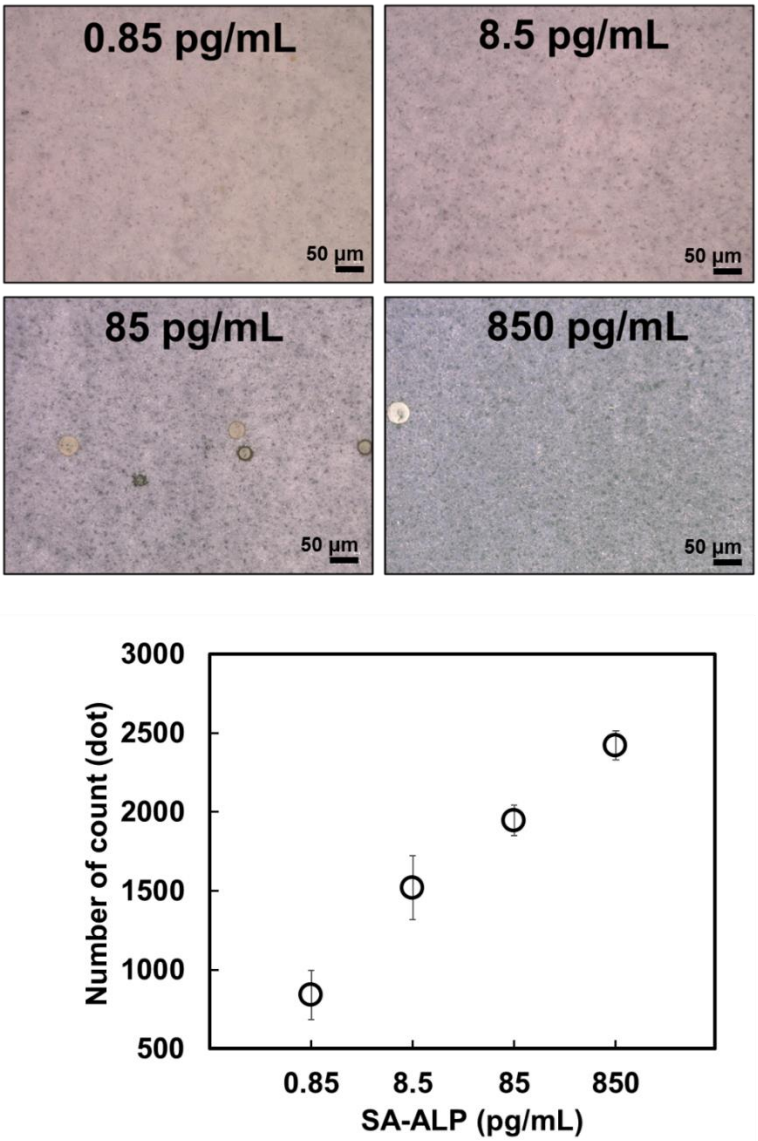

Figure 3.4.3.2 Microscopic images of the test zone of µPADs and the corresponding number of count (dot) response. The experiment was carried out at 70 µL of different concentration of SA-ALP (0.85 to 850 pg/mL) containing 0.1% v/v BSA in substrate buffer. The test zone was 0.5 mg/mL biotin-BSA at 0.3 µL. The test zone was incubated in 2.5 µL BCIP/NBT substrate (1:4 dilution) at for 48 h incubation.

3.5 Conclusion

In this chapter, single-molecule detection without the use of an ultra-small chamber for digital counting on a µPAD was demonstrated. Digital counting of amplified signal as dots was successfully done on µPAD by a simple enzymatic reaction system that produced insoluble color. A better visualization of dots was obtained by allowing incubation in sufficient time inside the moist plastic box. The sensitivity of µPAD at single-molecule level was achieved by digital counting visible dots which indicated the present of molecules. Finally, the proposed method was used to determine SA-ALP molecules from 0.85 to 850 pg/mL using inexpensive materials and general laboratory equipment. This demonstration has shown the potential to advance sensitivity of µPAD to the single-molecule detection. The higher sensitivity of µPADs will allow more users to detect lower concentration of their biomolecule target in variety of analytical applications than they ever could. When biomarker can be detected in their earliest stages, especially before symptoms/damage even appear, there is a higher chance for proper treatment, saving lives and preventing spread of problems. Future work focusing on decreasing the reaction time and automating the detection procedure is expected to improve the potential for practical on-site application.

3.6 References

[1] S.M. Schubert, L.M. Arendt, W. Zhou, S. Baig, S.R. Walter, R.J. Buchsbaum, C. Kuperwasser, D.R. Walt, Ultra-sensitive protein detection via Single Molecule Arrays towards early stage cancer monitoring, Scientific reports, 5 (2015) 11034-11034.

[2] N. Momenbeitollahi, T. Cloet, H. Li, Pushing the detection limits: strategies towards highly sensitive optical-based protein detection, Analytical and Bioanalytical Chemistry, 413 (2021) 5995-6011.

[3] A. Apilux, Y. Ukita, M. Chikae, O. Chailapakul, Y. Takamura, Development of automated paper-based devices for sequential multistep sandwich enzyme-linked immunosorbent assays using inkjet printing, Lab on a Chip, 13 (2013) 126-135.

[4] S. Charernchai, M. Chikae, T.T. Phan, W. Wonsawat, D. Hirose, Y. Takamura, Automated Paper-Based Femtogram Sensing Device for Competitive Enzyme-Linked Immunosorbent Assay of Aflatoxin B1 Using Submicroliter Samples, Analytical Chemistry, 94 (2022) 5099-5105.

[5] D.M. Rissin, C.W. Kan, T.G. Campbell, S.C. Howes, D.R. Fournier, L. Song, T. Piech, P.P. Patel, L. Chang, A.J. Rivnak, E.P. Ferrell, J.D. Randall, G.K. Provuncher, D.R. Walt, D.C. Duffy, Single-molecule enzyme-linked immunosorbent assay detects serum proteins at subfemtomolar concentrations, Nature Biotechnology, 28 (2010) 595-599.

[6] Y. Rondelez, G. Tresset, K.V. Tabata, H. Arata, H. Fujita, S. Takeuchi, H. Noji, Microfabricated arrays of femtoliter chambers allow single molecule enzymology, Nature Biotechnology, 23 (2005) 361-365.

[7] K. Leirs, P. Tewari Kumar, D. Decrop, E. Pérez-Ruiz, P. Leblebici, B. Van Kelst, G. Compernolle, H. Meeuws, L. Van Wesenbeeck, O. Lagatie, L. Stuyver, A. Gils, J. Lammertyn, D. Spasic, Bioassay Development for Ultrasensitive Detection of Influenza A Nucleoprotein Using Digital ELISA, Analytical Chemistry, 88 (2016) 8450-8458.

[8] H. Liu, Y. Lei, A critical review: Recent advances in "digital" biomolecule detection with single copy sensitivity, Biosens Bioelectron, 177 (2021) 112901-112901.

[9] B.D. Grant, C.A. Smith, K. Karvonen, R. Richards-Kortum, Highly Sensitive Two-Dimensional Paper Network Incorporating Biotin–Streptavidin for the Detection of Malaria, Analytical Chemistry, 88 (2016) 2553-2557.

[10] P. Preechakasedkit, W. Siangproh, N. Khongchareonporn, N. Ngamrojanavanich, O. Chailapakul, Development of an automated wax-printed paper-based lateral flow device for alpha-fetoprotein enzyme-linked immunosorbent assay, Biosensors and Bioelectronics, 102 (2018) 27-32.

[11] A. Trinh le, M.D. McCutchen, M. Bonner-Fraser, S.E. Fraser, L.A. Bumm, D.W. McCauley, Fluorescent in situ hybridization employing the conventional NBT/BCIP chromogenic stain, BioTechniques, 42 (2007) 756-759.

CHAPTER IV

GENERAL CONCLUSION

In this study, a high-sensitive immunoassay approach on microfluidic paper-based analytical devices (µPADs) has been successfully developed for both analog and digital counting.

To improve the sensitivity of analog counting µPADs for competitive enzyme linked immunosorbent assay (ELISA) of small molecule detection, the device was successfully developed to demonstrate Aflatoxin B_1 (AFB_1) measurement. The new finding of a novel sample-loading method: dropping sample solution into the zones that had been prepared with an antibody-conjugated enzyme, followed by immersion in a running buffer, allowed the improved reaction and sensitivity while simultaneously minimizing the sample volume.

The digital counting was successfully demonstrated on a colorimetric enzymatic- µPAD. Through software processing on microscopic images, the proposed method shows the potential in digitally count streptavidin-conjugated alkaline phosphatase (SA-ALP) molecules at the picogram level (0.85 to 850 pg/mL).

For future work, the paper and glass substrate are expected to be applied to bridge-amplification with digital fluorescence signal counting for improving the sensitivity and detection assay time of single molecule detection.

LIST OF PUBLICATIONS

Journals

S. Charernchai, M. Chikae, P. T. Tue, W. Wonsawat, D. Hirose, Y. Takamura, Automated Paper-Based Femtogram Sensing Device for Competitive Enzyme-Linked Immunosorbent Assay of Aflatoxin B1 Using Submicroliter Samples, Analytical Chemistry 2022, 94 (12), 5099-5105.

International conferences

1. **S. Charernchai**, M. Chikae, W. Wonsawat, D. Hirose, P. T. Tue, Y. Takamura, Development of laser-cut microfluidic paper-based analytical device with sucrose valves for automated competitive ELISA of Aflatoxin B_1 detection, The Twenty Third International Conference on Miniaturized Systems for Chemistry and Life Sciences (μTAS 2019), Switzerland, October 27-31, 2019. (**Poster presentation**)

2. **S. Charernchai**, M. Chikae, W. Wonsawat, D. Hirose, Y. Takamura, A low-volume sample and high sensitive microfluidic paper-based analytical device integrated sucrose valve for automated competitive ELISA of Aflatoxin B_1 detection, The Twenty Fifth International Conference on Miniaturized Systems for Chemistry and Life Sciences (μTAS 2021), United States, October 10-14, 2021. (**Poster Presentation**, online)

Domestic conferences:

1. **S. Charernchai**, M. Chikae, W. Wonsawat, D. Hirose, Y. Takamura, Automated paper-based femtogram sensing device for competitive enzyme-linked immunosorbent assay of Aflatoxin B_1 using sub-microliter samples, The 69^{th} JSAP Autumn Spring, Tokyo, March 22-26, 2022. (**Oral presentation**, online)